1-1-2012

Design And Testing Validation Of An Extendable Pressurized Tunnel For An Inflatable Lunar Habitat

Timothy Jani Holland

DESIGN AND TESTING VALIDATION OF AN EXTENDABLE PRESSURIZED TUNNEL FOR AN
INFLATABLE LUNAR HABITAT

By

Timothy Jani Holland

Bachelor of Science, Syracuse University 2010

A Thesis

Submitted to the Graduate Faculty

Of the

University of North Dakota

In partial fulfillment of the requirements
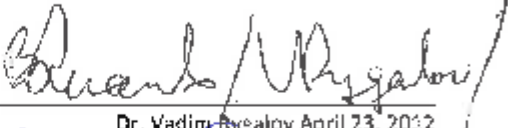

For the degree of

Master of Science

Grand Forks, North Dakota
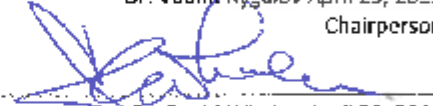
May

2012

This thesis, submitted by Timothy Jani Holland in partial fulfillment of the requirements for the Degree of Master of Science from the University of North Dakota, has been read by the Faculty Advisory Committee under whom the work has been done and hereby approved.

_____
Dr. Vadim Rygalov April 23, 2012
Chairperson

_____
Dr. David Whalen April 23, 2012

_____
Dr. Reza Fazel-Rezai April 23, 2012

This thesis meets the standards for appearance, conforms to the style and format requirements of the Graduate School of the University of North Dakota, and is hereby approved.

_____
Dr. Wayne Swisher
Dean of the Graduate School

April 23, 2012_____
Date

PERMISSION

Title: Design and Testing Validation of an Extendable Pressurized Tunnel for an Inflatable Lunar Habitat

Department: Space Studies

Degree: Master of Science

In presenting this thesis in partial fulfillment of the requirements for a graduate degree from the University of North Dakota, I agree that the library of this University shall make it freely available for inspection. I further agree that permission for extensive copying for scholarly purposes may be granted by the professor who supervised my thesis work or, in her absence, by the chairperson of the department or the dean of the Graduate School. It is understood that any copying or publication or other use of this thesis or part thereof for financial gain shall not be allowed without my written permission. It is also understood that due recognition shall be given to me and to the University of North Dakota in any scholarly use which may be made of any material in my thesis**.**

Signature   Timothy J. Holland

Date   April 23, 2012

TABLE OF CONTENTS

LIST OF FIGURES

Figure   Page

LIST OF TABLES

Acknowledgments

The author expresses sincere appreciation to Senior Research Associate Pablo de Leon, for pointing out all of his mistakes and working with the author to solve all of them.

The author expresses sincere appreciation to Tyler Jacobson for his expertise in welding to fabricate components when time was an essence.

The author expresses sincere appreciation to his Master's Thesis Committee participants: Dr. Vadim Rygalov, Dr. David Whalen, and Dr. Reza Fazel-Rezai.

The author expresses sincere appreciation to the UND Space Studies Department for opportunity to conduct this research.

To Dr. John W. Holland

ABSTRACT

In the design of the UND inflatable lunar habitat (ILH), the need for an extendable pressurized tunnel to link the habitat to a wheeled terrestrial vehicle (rover), and secure the connection between both elements is one of the critical problems to be solved in order to test the validity of the ILH concept. The design of an extendable pressurized tunnel is required in order to allow access to and from the rover without the use of pressure suits. It is expected than using an extendable tunnel will allow simple docking procedures. An experimental process is required to determine the best procedure to dock the pressurized rover with the habitat.   This will be done by a number of tests to determine the docking position. Testing of the docking element, extension units, and docking position will be required. This will prove that this design of an extendable pressurized tunnel is a valid solution to the problem.

CHAPTER I

INTRODUCTION

Space is a hostile environment for humans. It is a vacuum, lacks a breathable atmosphere, and has extreme temperature changes depending on position relative to the Sun. For humans to survive in space, they need to bring an Earth-like environment with them. This means a life support system to supply breathable air, pressure, water, and food. This Earth-like environment has to be contained so it does not escape into the vacuum of space. This is where the need for a space habitat comes into play. The space habitat contains the livable Earth-like environment, and the much needed life support system. A space habitat has to be more than just a barrier between the Earth-like environment and the vacuum of space; it also has to contain the hardware needed for the humans to complete their mission of exploration: with living quarters, laboratories, maintenance facilities, and support systems. The proof-of-concept design of the UND Human Spaceflight Lab's Inflatable Lunar Habitat (ILH), Pressurized Electric Rover (PER), and suitport analog setup will help research in this area of life support on planetary bodies.

There are three main research areas for the analog Lunar Habitat system:

1. Testing of proof-of-concept hardware: such as the suitport, pressurized tunnel, NDX-1, NDX-2, etc.

2. Human Factors research: crew selection, training, psychosocial interaction, habitat design, human-machine interaction, etc.

3. Scientific research in fields that relate to planetary exploration: geology, biology, and other fields of science

This thesis is addresses the first area and in particular the issue of how to transfer from the ILH to the PER without the need for the crew to wear pressure suits. To understand the need for a transfer system between the ILH and the PER, a look at past examples of spacecraft mating systems is warranted. Also current technology in the field has to be discussed to find out what current capabilities for this transfer system are. An explanation of what analog testing can do for future space exploration all has to be taken into account before the design of the transfer system can be discussed. The method of the design is as important as the design itself. This thesis will go into the testing phase of the transfer system. Only the preliminary testing will be done in time for this thesis, but it will open up future research using the hardware systems that this work describes. At the end of this thesis it will be shown that a working prototype of the transfer system and preliminary testing of it has been accomplished.

Why go back to the Moon?

Humans have already been to the Moon. That was the prize of the space race and the goal of the premier American civil space program, Apollo, under the guidance of the National Aeronautics and Space Administration (NASA). Why should humans return where they have already been? There are a number of reasons to go back to the Moon. The short list includes: accessibility, inspiration, international cooperation, geology,

study of asteroid threat, astronomy, energy production, resources, technology, and as a stepping stone for further solar system exploration.

The Moon orbits Earth at a relatively small distance compared to any other planetary body, at an average distance of 233,000 miles or 375,000 km. Using Apollo Era technology, it only took three days to get there.   With current technology it should take about the same length of time.

It is part of human nature to want to explore; whether it is the Moon, the new restaurant down the street, or a national park. A lunar base will stimulate the interest of science and engineering in the youth of the world just as Apollo did when men walked on the Moon (Ruess, Schaenzlin, & Benaroya, 2006).

The International Space Station is a great example of what a combined international effort can accomplish. To have a few different organizations all set up their own lunar bases would be unnecessarily redundant and only have a limited scope (Ruess, Schaenzlin, & Benaroya, 2006). Space treaties have been enacted under international law to provide that development should be for a peaceful effort for the benefit of all people of Earth.

The Apollo missions answered a great number of questions about the Moon, but they also opened up many more questions that still need answers. A lunar base would benefit not only planetary scientists, who are interested in lunar geology, but a wide range of sciences such as: biology, physics, paleontology, psychology and sociology.

The impact of asteroids on Earth would not be very good for humans; they have the potential to wipe off all life on the planet.   The Moon has billions of years of impacts preserved on its surface. This could allow scientists to figure out if mass extinctions on Earth were the result of a single large asteroid impact or lots of smaller asteroids impacts or some other feature (Ruess, Schaenzlin, & Benaroya, 2006).   A lunar base could also ensure the survival of the human race if something happens to the Planet Earth.

Large optical telescopes, much bigger than Hubble, could be built on the Moon without worry of light being scattered due to atmosphere. Radio telescopes could be built on the far side of the Moon and shielded from the radio noise from Earth (Ruess, Schaenzlin, & Benaroya, 2006). Working in the 1/6 Earth's gravity on the lunar surface would make it much easier to service the telescopes then if they were in micro-gravity or zero gravity out in space or low Earth orbit (LEO).

Setting up solar panels on the Moon which convert sunlight to electric power, then beaming that power to the Earth could be used to help stop the world's dependence on fossil fuels (Ruess, Schaenzlin, & Benaroya, 2006).

The lunar regolith has iron, aluminum, titanium, oxygen, and traces of hydrogen, carbon, helium3, and nitrogen in it (Ruess, Schaenzlin, & Benaroya, 2006). There is also water on the Moon. These resources could be used to produce rocket fuel and the Moon could be used as a base for further exploration of the solar system.

The exploration of space has created many spin-offs that benefit economies and societies; continued exploration will expand this. A lunar base will create business opportunities and jobs for people in many different fields (Ruess, Schaenzlin, & Benaroya, 2006). A lunar base once fully running could be used as a test bed for advanced technologies such as in-situ resource utilization, electromagnetic propulsion, and life-support systems.

A lunar base would make a great test bed for future advanced technologies and as a launch area for heavy spacecraft to the red planet.

Lunar Environment

The lunar environment is very different from Earth's environment: gravity, vacuum, radiation, and temperature are all challenges that have to be overcome. On the Moon, gravity is $1/6^{th}$ of what it is here on Earth. The lunar surface is exposed to a vacuum, meaning there is no atmosphere, no wind, no weather, but also no pressure or breathable air. Depending on whether the lunar surface is exposed to the lunar night or lunar day, temperatures can vary from 100 to -150 degrees Celsius. Radiation is a much bigger concern on the Moon because there is no atmosphere or Van Allen belts to protect the Moon. Impacts are also a problem; from micrometeoroids to asteroids, the lunar surface has evidence that it has been hit before.

Analog Testing for Space

Analog testing is important for the exploration of space. Analog testing is done in an area that is realistic to a surface of another planetary body such as the Moon or Mars. Extreme environments on Earth help to test designs of facilities and operations for extraterrestrial environments (Bannova).   This allows integrated systems to be tested that involve cargo and human landers, lunar habitats, unpressurized rovers, pressurized rovers, robotic systems, extra-vehicular activity (EVA) test subjects, EVA tool repairs, and operational performance of space hardware.   These analog missions are treated as the real thing by simulating regolith, navigation and communication systems, emergency response scenario development, and duration testing (Chambers & Fischer, 2011). There is a history of analog testing throughout the development of space exploration.

History of Analog Testing

Analog testing for human exploration was started with the Apollo program in the 1960s. These analog missions were called Geology Field Trips (GFTs) and were conducted at remote locations that were chosen because the geology, terrain, or climate characteristics that was similar to the lunar surface (Loff & Lind, Past and Present: Field Testing For the Moon, 2009). In 1963 NASA astronauts Buzz Adrin, Neil Armstrong and Michael Collins went outside of Flagstaff, AZ to practice sample collection with special tools and practice with communication systems that they would use on the moon in 1969 (Loff & Lind, Past and Present: Field Testing For the Moon,

2009). The GFTs included locations such as Hawaii, Minnesota, Nevada, New Mexico,

Texas, Washington, the Grand Canyon, Canada, Iceland and Panama. Each GFT has its

own goals for the mission, such as identifying rock formations, sample recovery, survival

training, and communication techniques.   GFTs ended in 1972 when NASA's Moon

missions were canceled.

Figure 1: Apollo 16 astronauts John W. Young and Charles M. Duke Jr., study rock formations along their simulated lunar traverse route from http://www.nasa.gov/exploration/analogs/then-and-now.html

Now more than 40 years after the last person was on the Moon, analog missions

for Mars or the Moon have been conducted by numerous groups, many sponsored by

NASA, but others are privately funded. Analog testing has greatly expanded from GFTs

to intense simulation missions with everything from robots and rovers to delayed

communication times.   One example of an improvement that recent analog testing has

come up with is the Planetary Aid for Traversing Humans (PATH) under development at

Massachusetts Institute of Technology. With the PATH system applied to a planetary

EVA to help make real-time decisions about the EVA to get the most out of the time of

the EVA (Marquez & Newman, 2006). Using PATH allows the astronaut to make

informed decisions of how long each task will take and how much time they have to

spend on it. This allows the astronaut to use this data to make an informed decision of

how to best spend the limited amount of EVA time to get the most important tasks done.

<p style="text-align: center;">***Analog Test Sites/Missions/Teams***</p>

Analog test sites and teams are scattered all over the world from numerous countries and space agencies. This paper will only focus on the American civil space program under the direction of NASA.

NASA Desert Rats

NASA's Desert Research and Technology Studies (RATS) team is a group that meets every year in the Arizona desert to test human-robotic systems and extravehicular equipment and establishes requirements for operations and procedures. This creates a knowledge base that helps scientists and engineers design, build, and operate better equipment for the environment they expect to run into on another planetary body (Loff & Lind, Desert RATS, 2012). This is NASA's main analog program; all of its big name projects are tested during the annual missions.

Haughton-Mars Project

The Haughton-Mars Project (HMP) is based in the Haughton crater on Devon Island in the High Arctic. This terrain is seen as a terrestrial analog for the surface of Mars. HMP is a test area for an exploration program aimed at developing new technologies, operational procedures, human factors experience for future space

exploration (Lee & Lorber, 2010). This is an international research station that is run and owned by the Mars Society.

Pavilion Lake

The Pavilion Lake Research Project (PLRP) is based in the underwater environment of Kelly Lake, British Columbia, Canada. PLRP's focus is on science and science operations using DeepWorker submersibles to explore, study, and document rare freshwater carbonate rock formations. Using real field science procedures, scientists are learning about how to conduct safe, productive and discovery-based science in extreme environments and apply this knowledge to future space exploration (Loff & Lind, Pavilion Lake Team Explores the Deep to Learn More about Life and Science, 2011).

NEEMO

The NASA Extreme Environment Mission Operations (NEEMO) project is analog missions that take place 62 feet (19 meters) below the surface of the water off the coast of the Florida keys in an underwater laboratory called Aquarius (Kauderer & Dunbar, 2011).   Aquarius is owned by the National Oceanic and Atmospheric Administration and managed by the University of North Carolina at Wilmington.   Marine biologists usually use Aquarius as a home base as they study the coral reef. Aquarius has lab equipment and computers inside it that allow scientists to perform research and process data samples without returning to the surface or leaving their home base. Starting in 2001 NEEMO has completed 15 missions at Aquarius primarily for astronaut training and

testing equipment and operational concepts for space exploration (Kauderer & Dunbar, 2011). Mission 15 the most recent mission which tested equipment and operations for the exploration of a near-Earth asteroid (NEA), before it was cut short because of a hurricane.

Inflatable Lunar Habitat

In Antarctica at the McMurdo Station which is isolated from the rest of the world, an analog mission was run to evaluate how easily a suited astronaut could assemble, pack, and transport an inflatable lunar habitat (Loff & Lind, About Analog Missions And Field Tests, 2011). The purpose of this mission was to test if an inflatable lunar habitat could be used on the Moon, which would reduce the amount of hardware and fuel necessary for transportation and logistics on the Moon.

Moses Lake, WA

Moses Lake, WA has sand dunes, rugged terrain, soil inconsistencies, sandstorms, and temperature swings to make it a good site for analog space testing. The short distance mobility exploration engineering evaluation analog field tests were to compare the advantages of using pressurized vehicles versus unpressurized vehicles (Loff & Lind, About Analog Missions And Field Tests, 2011).

Black Point Lava Flow, AZ

The lava flow terrain of Black Point Lava Flow, AZ is an environment geologically similar to the lunar surface. NASA tested pressurized rovers here to see if they could

function in the rough terrain and to have an idea of how they would perform on the lunar surface (Loff & Lind, About Analog Missions And Field Tests, 2011).

Volcanic Terrains in Hawaii

Hawaii's islands have volcanic terrain, rock distribution and soil composition in an ideal environment for testing hardware and operations which could function on the moon. NASA mainly tests hardware and processes that use in-situ resources to support human and robotic exploration such as end-to-end oxygen extraction, separation, and storage from the volcanic material (Loff & Lind, About Analog Missions And Field Tests, 2011).

Inflatable Lunar Habitat

The UND Inflatable Lunar Habitat (ILH) is designed to support a crew of 4 for 30 days in an analog mission to the moon, which will take place in the Badlands in west North Dakota. The ILH is 40 feet long and 11 feet wide. As it is shown in Figure 2 the frame of the ILH is a steel structure to support the weight, and to withstand the stresses of transportation across the state and back. On a non-Earth planetary surface the steel will be replaced by composite materials to provide structure.
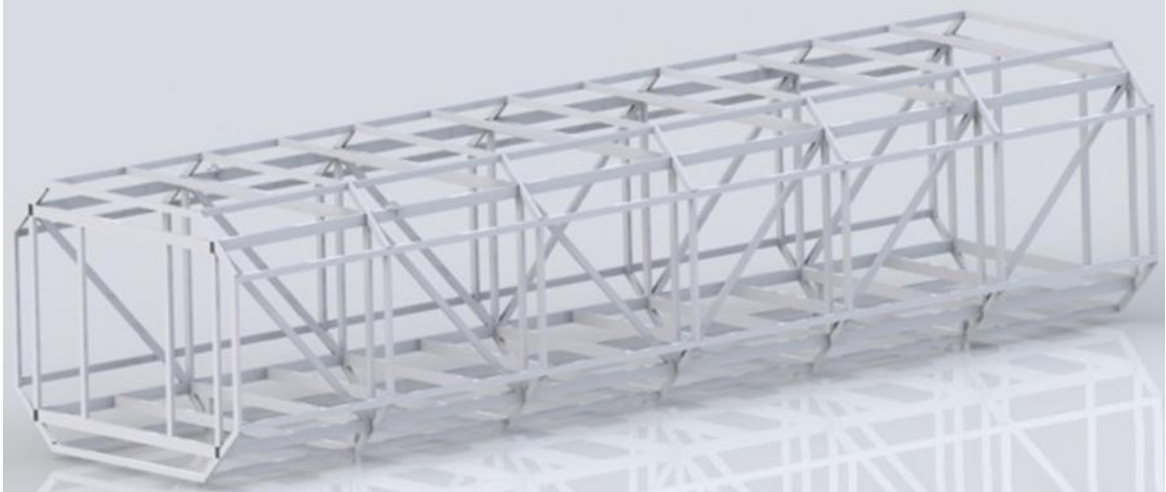
Figure 2: Steel Support Structure of ILH, drawing by David Booth

The interior of the ILH will have 4 individual crew quarters, a laboratory, a bathroom, and a galley. One end of the ILH is the laboratory and a center isle goes down the rest of the ILH that leads past the bathroom, galley, and the four crew quarters.

The ILH is important to the success of the mission. A number of issues have to be addressed by the ILH to ensure physical and mental health of the crew. The longer the mission is; the more crew privacy and recreation is required. The human body will de-condition in gravity less than Earth's, this includes the Moon and Mars, but not as quickly as in microgravity (Kennedy, Toups, & Smitherman, 2007). For an analog mission, this does not be needed to be taken into account.   For missions lasting up to six months, crews require their own private personal quarters for sleeping as well as private recreation such as reading, writing or watching a movie without interacting with the rest of the crew, while for longer missions crew members will require more private areas such as dressing areas, sitting areas, and more complete recreational and exercise

facilities (Kennedy, Toups, & Smitherman, 2007).   There are also a number of common

requirements of a space habitat:

1. Acceptable physiological and psychological support for humans

2. Successful accommodation of mission objectives

3. Reliable structural integrity with adequate safety margins

4. Forgiving failure modes such as leak before rupture

5. Ability to be tested to a high level of confidence before being put into service

6. Ability to be integrated with available launch systems

7. Straightforward outfitting and servicing

8. Easily maintained

9. Long design life

10. Commonality at the system or subsystem level

11. Basic physiological human needs: food, water, oxygen, personal hygiene, waste

    management

    The UND ILH has been designed to meet all of these requirements that relate to

analog mission operations.   More information of this ILH can be found in Lynn van

Broock's SpSt 593 Individual Research Study: Basic requirements of life support of a

Hybrid Inflatable Terrestrial Habitat as a first step in Lunar Habitation Strategies (van

Brook, 2010).

Pressurized Electric Rover

The Pressurized Electric Rover (PER) is an important part of the analog mission. The PER allows exploration and transportation in a shirtsleeves environment, one that does not require the astronaut to be in a space suit. This is different than the rover that the Apollo missions drove on the Moon, those rovers were unpressurized and required the astronauts to be in spacesuits.   The PER also will have the suitport system attached to the back of the rover. The PER is design to hold two crew members, but be able to house four in an emergency. It is to be used for surface operations on a planetary body. It can be used to assist in data and samples collection, transportation between station, and exploration.

Figure 3: Photo of PER behind Ryan Hall on the Campus of the School of Aerospace at UND

Figure 4: Drawing of PER by Wataru Suzuki

Figure 4 shows the design of the PER and Figure 3 the built PER.

Transfer Problem between the Two Modules

There needs to be a way to transfer crew and cargo between the PER and the ILH without the use of space suits. A closed pressurized transfer system will help maintain habitat integrity, minimize leaks during transit phases, and limit dust in living compartments. Figure 5 below illustrates this need.
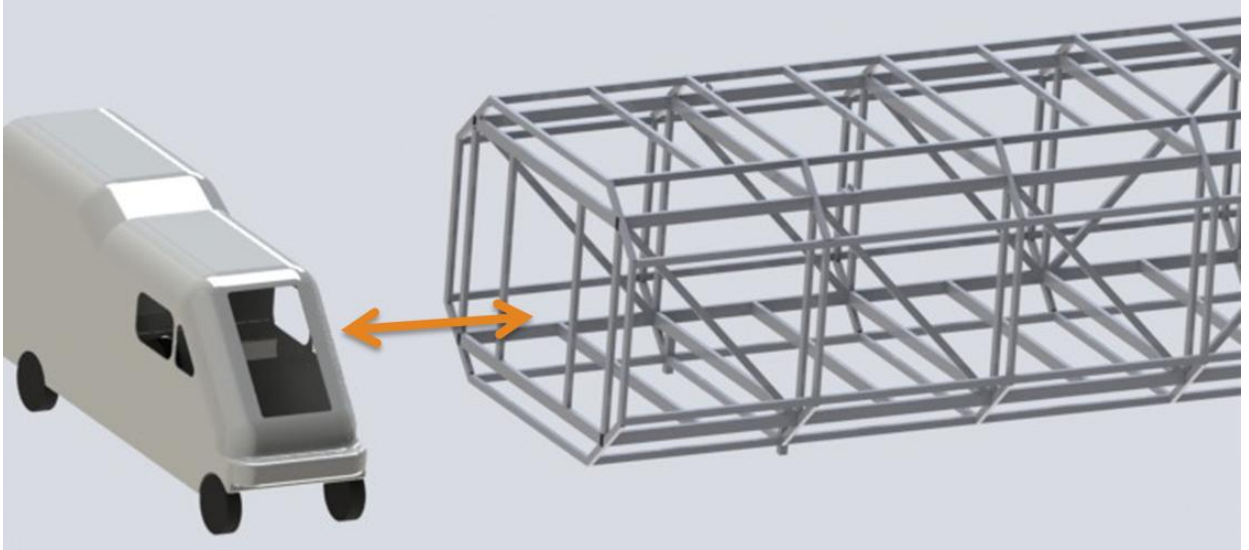
Figure 5: Transfer between PER and ILH drawing by Timothy Holland

Integrity

The ILH, PER, NDX-1, and NDX-2; all contain a livable environment for humans.

Life support systems supply this. It is most efficient to keep as much of the environment

inside the habitat. To do this all sources of leaks must be minimized. One main area for

leaks is during the transfer phase between the PER and ILH. Any transfer system has to

be designed to minimize leaks.

For any inflatable object there has to be a bladder to contain the air and pressure inside

it. The ILH is no different. The ILH has a bladder similar to that of a space suit. The

bladder has three main layers of fabric. The inner layer, which is the bladder, is there to

contain the internal environment. The middle layer is called the restraint layer. This

layer's job is to hold the bladder in the shape needed to keep the overall shape and

function of the spacesuit, habitat, or transfer system. The outermost layer is called the

thermal and dust protection layer. Its job on an Earth-analog environment is to insulate and protect the bladder and restraint layer from corrosion from dust, weather, and wind. On either side of the transfer system there has to be a gasket to seal the bladder to the metal elements.

Dust Issues on Planetary Surfaces

Dust on planetary surfaces causes numerous problems for humans.   Dust can coat equipment, short out electronics, can cause health problems when inhaled, damage equipment that is exposed to it.

Ultra-fine dust exists in an extremely thin and dry atmosphere like the one found on Mars (Mosher, 2007). "*If you walk through, pick up or simply touch the dust, it would gather charge and stick to you. We've already seen this on the rovers' wheels*," said Geoffrey Landis, a physicist with the NASA Glenn Research Center in Cleveland, Ohio. "*Things get even more interesting when winds come by and separate the charge*," (Mosher, 2007). Astronauts on Mars would become walking electric fields and attract even more dust to their spacesuits. "*The theoretical phenomenon is known as the triboelectric effect and is similar to the current generated while walking across a carpet floor during the winter, when the air is extremely dry and can't soak up static charge well*," (Mosher, 2007). This makes dust harder to deal with when cleaning the spacesuit to enter the habitat. Because of this triboelectric effect, dust can coat equipment and even cause static shocks which could damage electronics in a spacesuit or spacecraft.

The ultra-fine dust found on the Moon and Mars can cause a problem for astronauts when they inhale it. The smaller the dust particles are, the more likely that they can go deep into the lungs of an astronaut. On the Moon and Mars where both have reduced gravity compared to Earth's it may allow dust to hang around in living spaces longer and penetrate more deeply into astronauts' lungs if the dust particles are small enough (Mosher, 2007).

The best way to protect astronauts from Moon and Mars dust is not to expose astronauts to it. For the purpose of the ILH and PER project this was resolved by the suitport system and a transfer system that does not require the astronauts to enter the ILH with their spacesuits on.

Docking and Berthing

A specific vocabulary is used to define the docking and berthing processes. It is important to understand the meaning of these terms.

The GNC system is the Guidance, Navigation, and Control system that provide the means for the spacecraft to go to its desired orbit and position by use of different sensors, control software, and thrusters (NASA, 2000).

Mating is the general term used to describe the process of achieving contact, capture, and connection. Mating includes the two cases of docking and berthing.

The term docking is used to describe when the GNC system of the chaser spacecraft maneuvers it to the correct parameters to allow its capture interfaces to enter those of the target spacecraft, and where the location of the capture system is also the location that structural connection happens (Fehse, 2003).

Berthing is the term to describe the case where the GNC system of the chaser maneuvers the chaser to a position with nominal relative velocities and angular rates to the target, and a manipulator creates a capture between the two, and the manipulator transfers the captured vehicle to a final position to allow it connection between the two craft. In berthing operation the location for capture is different for the location that structural connection happens.

Docking Operations

In the docking process there are a number of steps that occur in order. The following steps are from a typical pressurized docking operation scenario. Pressurized docking operations are used for manned spacecraft. Figure 6 shown below is a diagram of the alignment and motion parameters at a docking. Compare this to Figure 7 to see the difference between docking and berthing.
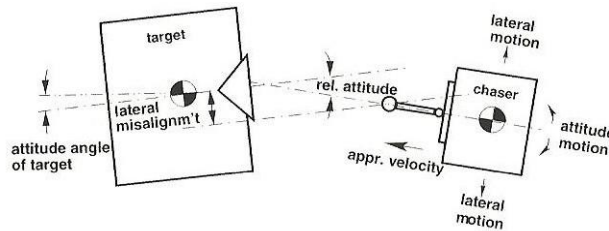
Figure 6: Alignment and motion parameters at docking contact (Fehse, 2003)

Table 1: Docking Operation Steps

Step	Main Action of Step	Details
Step 1	Reduction of the Approach Velocity and Correct Misalignments	The chaser aligns itself with the target to allow the docking interfaces of the target and chaser to interact
Step 2	Reception of the Chaser	Docking interfaces of the chaser and target are in range of each other. This is called the reception range. Reception range takes into account all residual dispersions of the chaser with respect to the target and all rebound motion that may take place after first contact before complete capture
Step 3	Impact Attenuation	Spring-damper devices will be applied to prevent any rebound from the interface structures of the two vehicles and creating a change of velocity that could misalign the docking process
Step 4	Capture	The two vehicles are in the reception range and the interface structures of both vehicles can guide each other into the conditions of alignment. Capture only means that the two vehicles cannot escape from one another, no rigid connection has been created.
Step 5	Retraction and Structural Alignment	The two vehicles are only loosely connected to one another. Any residual distance or lateral and/or angular misalignments will not allow the two to finish the docking process. A mechanical guiding feature is needed to improve alignment.

Step 6	Establish a Structural Connection	Engagement of structural latches to create a stiff structural connection and the two vehicles become one
Step 7	Utilities Connection	It can happen automatically or it can be done by the crew once the hatch is opened
Step 8	Pressurization	The volume enclosed between the two hatches is pressurized
Step 9	Hatch Opening	The hatches are opened

Berthing Operations

It does not matter which vehicle has the manipulator arm mounted on it, but for

the following example that is based on the International Space Station (ISS) scenario,

the arm is mounted on the target.
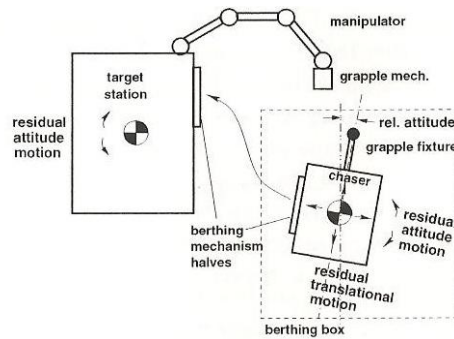
Figure 7: Berthing scenario: conditions at capture (Fehse, 2003)

Table 2: Berthing Operation Steps

Step	Main Action of Step	Details
1	Acquisition of Berthing Box by the Chaser	A berthing box is a volume of space near the target that the chaser has to be in to allow it to be captured by the grapple at the end of the manipulator arm
2	Acquisition of Readiness Position by the Manipulator arm	The arm is moved into a safe position, away from the berthing box, to be ready to capture the chaser
3	Switch-off of Chaser's Thrusters and Initiation of Capture	The chaser holds its position as the arm aligns with the grapple fixture on the chaser
4	Grappling of Capture Interfaces by the Manipulator	The arm's capture tool mates with the grapple fixture on the chaser, now the chaser cannot escape from the target
5	Transfer to the Berthing Port	The arm moves the chaser to allow it to align with the berthing hatch to allow for connection between the two vehicles
6	Alignment with the Berthing Port	The arm aligns the chaser with the berthing port
7	Establish a Structural Connection	Structural latches between the two vehicles are engaged to create a stiff structural connection, and the two vehicles

		become one
8	Utilities Connection	Done automatically or by the crew once the hatch is opened
9	Pressurization	The volume enclosed between the two hatches is pressurized
10	Hatch Opening	The hatches are opened

Docking Compared to Berthing

Docking is a very different operation from berthing. Both operations have similar steps to achieve the same goal of capture of the chaser vehicle to the target vehicle.

Docking has the attachment and capture interfaces on both the target and chaser vehicle. Docking requires the chaser vehicle to perform all the maneuvers to align itself to be in position to dock with the target vehicle.

In berthing operations the points for capture and attachment are at different areas of the spacecraft. Capture is determined by an arm on the target vehicle. This allows the target vehicle to have complete control of the capture and attachment of the chaser.

Docking operations are less complex, more reliable, less time consuming than berthing operations. Docking systems require more reception and damping systems then berthing systems. Berthing operations allows the movement of the chaser into positions that the chaser cannot align with because the arm can move the chaser differently than its own thrusters do.

Design Driving Requirements of Mating Systems

The design and size of the mating systems are determined by a number of driving requirements to fulfill the mission objectives.

One driving requirement is if the mating is for an unmanned mission or a manned mission. An unmanned mission does not require a pressurized transfer tunnel. An unpressured mating system is much simpler in design because it does not have to be air-tight (Fehse, 2003). Manned missions require a pressurized transfer tunnel.   The tunnel is to be formed after mating. The diameter of the docking or berthing mechanisms is dependent on the size of the tunnel required for transfer of goods and crew. This is usually the minimum cross section of the hatch and tunnel it is to allow passage of a crew member in a spacesuit (NASA, 1995).

The contact parameter is the necessary reception range that is determined by the lateral and angular misalignment between the two halves of the attachment mechanism at insertion, the half on the chaser, and the half on the target. The design and size of the contact mechanisms is determined by the relative translational velocities and angular rates at contact (Fehse, 2003). In docking operations this is determined by the guidance systems on the chaser vehicle. In berthing operations this is done by the guidance system of the arm moving the chaser into its target.

Utility lines are also a driving requirement. Utility lines provide power and air to pressurized vehicles. Utility connections can be performed by hand or automatically. The utility lines can connect outside the connection tunnel or within it. Either way, room must be left for the lines to connect the target to the chaser.

Figure 8 shows sizing features for a pressurized mating system. The inner diameter is big enough for a crew member in a space suit to go through the tunnel (Fehse, 2003).
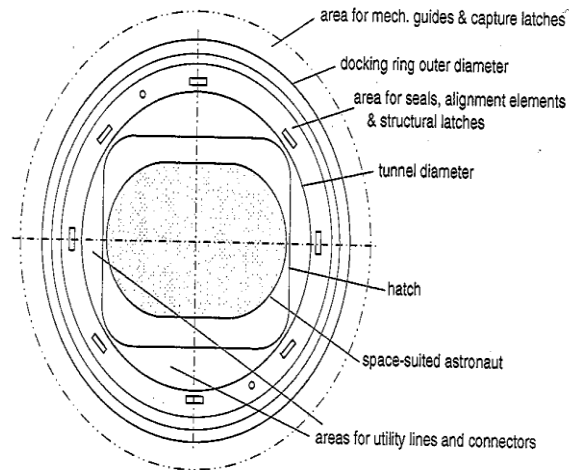
Figure 8: Sizing features for pressurized mating mechanisms (Fehse, 2003)

Central vs. Peripheral Docking Mechanisms

For docking systems, it is important for effective alignment of the chaser and the target spacecraft for capture at the first contact. This can most easily be implemented by a central capture mechanism. This is a rod on the side of the active vehicle or chaser, called a probe, with one end flexible and the other integrated into the structure of the

vehicle (Fehse, 2003). On the passive vehicle, or the target, there is a hollow cone, called a drogue that is used to receive the tip of the probe and guide it to the center of the cone, where capture can occur (Fehse, 2003). All early American and Russian space programs used this kind of capture method. The disadvantage of a central docking mechanism is that after the capture and hatch opening, the capture mechanism components, such as the probe and the drogue, have to be removed and stored somewhere else to allow transfer of goods and crew. Figure 9 shows a detailed diagram of how this system works.
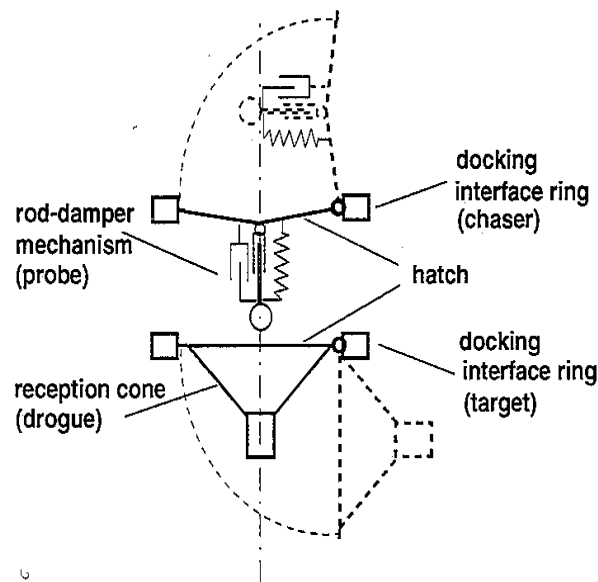
Figure 9: Central docking mechanism (Fehse, 2003)

To overcome the disadvantage of having to remove the central docking system setup, the idea of arranging the functional elements necessary for reception around the perimeter of the hatch was used. This will establish the transfer tunnel without having

to remove anything. This is known as a peripheral docking system. This is best shown in Figure 10.

This leaves the area inside the interface ring for passage of crew and goods, as only a flat hatch has to be open as shown in Figure 10. Peripheral attachment systems can also provide the ability for an androgynous design unlike a central docking system that has a male and female side. This androgynous design allows both the chaser and target to have capture and guidance systems. The first example of this design is the Apollo-Soyuz docking project in 1975.

Peripheral docking systems require a more complicated contact dynamics and shock attenuation system then a central docking system. This is because a peripheral docking system has its first contact point on a circle around the docking axis with a diameter of a meter or more. A three-dimensional model is needed to help understand the docking process. Using a central docking system the first contact happens at a

distance from the docking axis, this will create a situation that will require a few more contacts to dock the two.   The central docking system with its numerous contacts can have the contact dynamics figured out by the use of a two-dimensional model (Fehse, 2003). This is a much simpler process then what is required for the peripheral docking system.

Berthing systems do not require shock attenuation because of the slow velocity and full control at the final contact moment.

Androgynous design of docking mechanisms

Androgynous docking mechanisms have the same basic functions and interfaces on both sides of the docking unit. This allows either side to have the passive or active role in the docking process.   The primary objective is to provide increased operational flexibility for the spacecraft. A secondary advantage of this system is the increase in reliability over central docking systems due to the redundancy of having all the interfaces on both sides of the docking units. There is a price to pay for all of this, and it is the increase in weight of the vehicle. The more weight of the spacecraft, the less payload it can carry using the same amount of fuel.

Unpressurized docking/berthing mechanisms

If both vehicles that are going to mate are unmanned, then a pressurized transfer tunnel and all its supporting hardware is not required. This will reduce the weight of the mating system and the spacecraft. In a berthing system, the mechanism

can be reduced to the function of a structural connection latch (Fehse, 2003). In a

docking system, the shock attenuation and capture functions can be combined with the

structural connection function (Fehse, 2003).   See Figure 11. This is a V-latch used in

unpressurized docking and berthing operations.
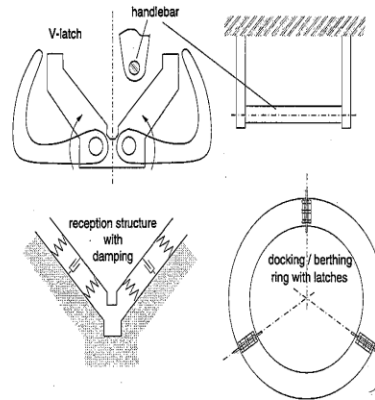
Figure 11: Unpressurised docking/berthing mechanism, V-latch (Fehse, 2003)

The V-latch system uses three to four latches arranged on the mating ring of the

active vehicle with handle bars as interfaces for the latches on the passive vehicle

(Fehse, 2003). The latch consists of a V-shaped structure to guide in the handlebar and

then pull the handlebar down to prevent escape. This secures the mating vehicles. This

type of mechanism has been used in space, most famously for the servicing and repair

missions for the Hubble Space Telescope.

Gemini Cone and Cup Docking System

Gemini VIII was the first mission to dock in space on March 16, 1966. The

docking was between a Gemini capsule spacecraft and an Agena spacecraft.   It was a

cone and cup docking system (Cook, Aksamentov, Hoffman, & Bruner, 2011). The male

end (the cup) was on the Gemini spacecraft, which was the chaser, and the female end was the cone on the Agena spacecraft, which was the target. The cone had a V-shaped notch which the Gemini used an indexing bar to align with.   This is shown in Figure 12.
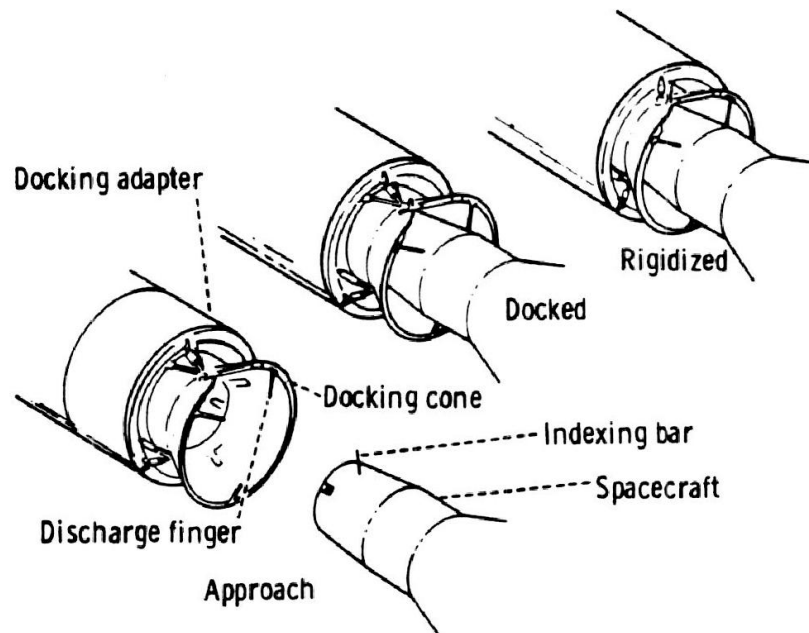
Figure 12: Overview of Gemini Docking Mechanism (Cook, Aksamentov, Hoffman, & Bruner, 2011)

"When the distance between vehicles was 250 miles radar was switched on. As the gap closed to 50 miles, the Gemini astronauts picked up the Agena's flashing beacon and took over control of Gemini. Aiding the astronauts was the status display panel outwardly mounted on the Agena-D, giving visual data on Agena fuel reserves, electrical power, and attitude position. During rendezvous maneuvers the relative speed between the vehicles was cut to less than 2 mph, so that when docking, their noses touched gently. On contact, the Gemini's narrow end entered the Agena's target docking adapter, whose latches clamped shut to prevent the two vehicles from slipping apart. Then a motorized Agena unit pulled the Gemini inward. Once the two craft were tightly

moored, matching electrical contacts met and gave the Gemini astronauts direct control

of Agena's onboard equipment - guidance, propulsion, attitude control, relay switches,

and the rest. Union of the two vehicles results in a Gemini /Agena spacecraft almost 50

feet long and much more versatile. The rocket power provided by Agena allowed for

flights to higher altitudes or to change orbital plane," (Cook, Aksamentov, Hoffman, &

Bruner, 2011).

Gemini VII proved that space docking could be done and this opened up the way

for the advancement of space exploration.

Apollo Probe-Drogue Docking System

The Apollo probe-drogue docking system is a central docking system. The Apollo

probe-drogue docking system uses a reception cone with a capture hole in the center on

the target side and a spherically suspended rod with shock attenuation on the chaser

side (Fehse, 2003). Once first contact occurs with the reception cone, the conical tip of

the rod on the chaser is pushed into the capture hole (Fehse, 2003). Once the tip of the

rod is in the capture hole, the rod retracts and pulls the target to the intended distance

to become a capture situation. An example of this can be seen in Figure 13.
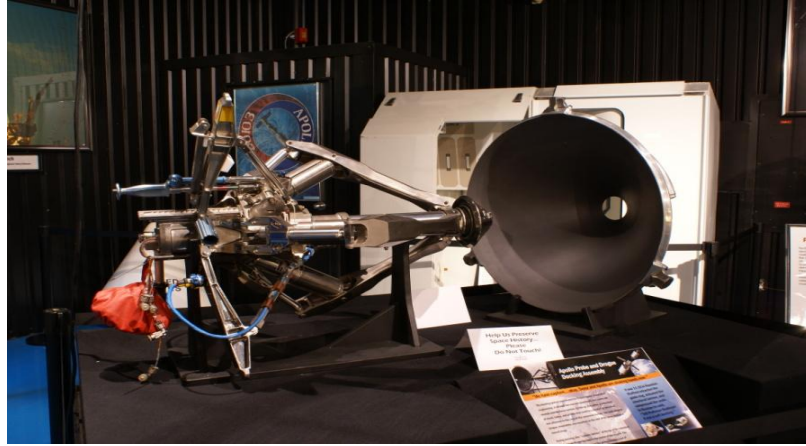
Figure 13: Apollo Probe-Drogue Docking System from http://heroicrelics.org/stafford/apollo-probe-and-drogue/dsc46571.jpg.html

Figure 14 shows the entire set-up of the Apollo docking system as the Command

Module docks with the Lunar Module.
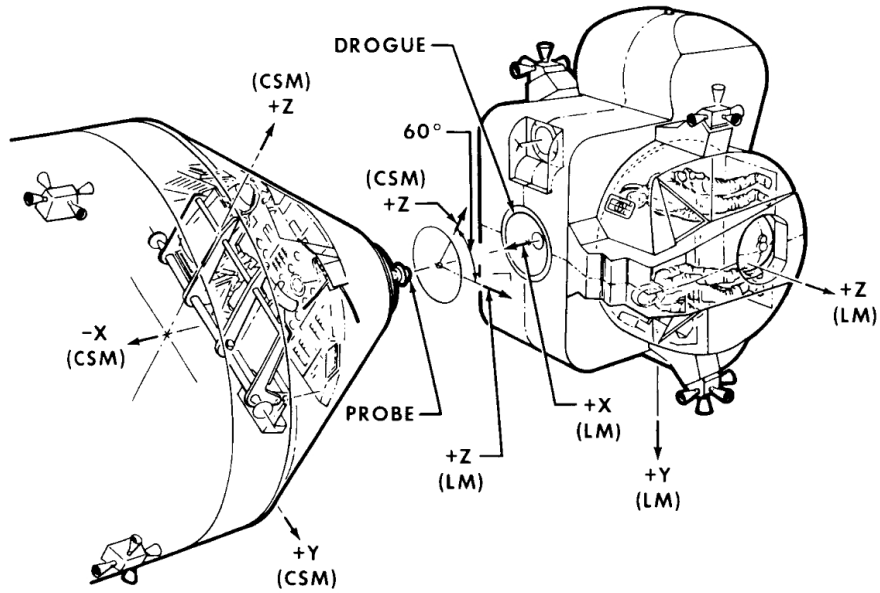
Figure 14: Apollo Spacecraft Docking (Cook, Aksamentov, Hoffman, & Bruner, 2011)

The Russian Probe-Drogue Docking System

This docking system has been used in the Salyut and Mir Space Station missions for the docking of the Soyuz and the unmanned Progress spacecraft. This system is very similar to the Apollo probe-drogue docking system. It is a central docking system. The reception cone and capture socket is on the target spacecraft and on the chaser there is a spherically suspended rod with shock attenuation (Fehse, 2003).

In 1962 Soviet engineers Viktor P. Legostayev and Vladimir S. Syromyatnikov started to design a pin-and-cone device to allow the Soyuz 7K to dock with the 9K propulsion module, and no internal transfer passageway was needed (Hall & Shayler, 2003). The probe, also called a pin, was designed to be the shock absorber that used sensors on its tip to signal when contact was made with the passive cone and turn off the control system on the active spacecraft. At the same time, the control system of the chaser would react with the signal from the sensors at the tip of the cone that would also tell the spacecraft to fire its thrusters to bring them together (Hall & Shayler, 2003). From 1971 the Soviet space station missions used an improved version of the 1962 model of the "pin-and-cone" that allowed its removal for the use of an internal transfer hatch.

Apollo-Soyuz Androgynous Peripheral Docking System

This is the original peripheral docking system. It was developed independently by the USA and the Soviet space agencies following a joint interface specification for the

joint Apollo-Soyuz mission in 1975. This was the first androgynous docking system ever

tested.

The docking occurs with one side assuming the active role, and the other the

passive role. First contact occurs at the flanks of the three guiding petals mounted on

the outside of each side's contact rings. These flaps are called petals because during

this process they fold like a flower closing its petals. On the active side the dampers are

extended and on the passive side they are retracted. Each petal has a spring-loaded

capture latch that will connect with a latch-catch on the opposite ring. Once contact

happens, the active contact ring will be pushed toward the passive contact ring to align

the capture latches that will engage to their corresponding catches. Once there is

capture, the contact ring for each side is retracted to create a structural connection

(Fehse, 2003). See Figure 15.
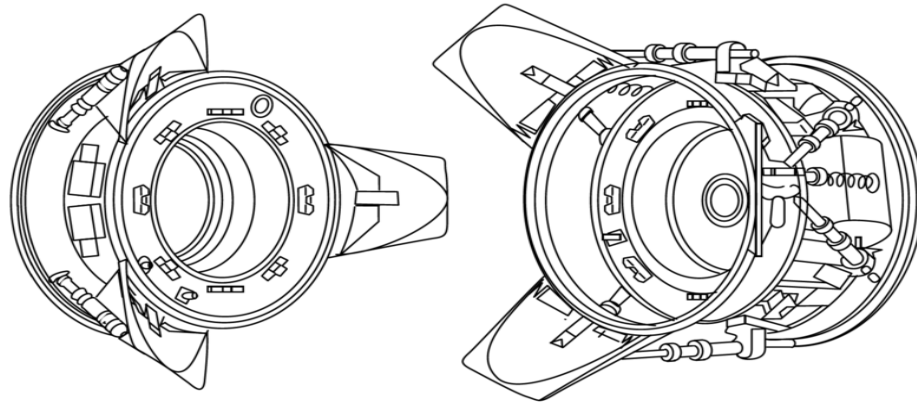
**Figure 15: Apollo-Soyuz docking mechanism assembly, USA on the left, Soviet on the right from
http://en.wikipedia.org/wiki/File:APAS-75_docking_system_drawing.png**

APDS: Androgynous Peripheral Docking System

The APDS is an updated version of the Apollo-Soyuz docking system. It was
designed for the Soviet Buran space shuttle, and was mounted on the Mir space station.
It underwent modifications to be used by the USA Space Shuttle for visits to Mir and
another one was mounted on the ISS (Fehse, 2003). See Figure 16.
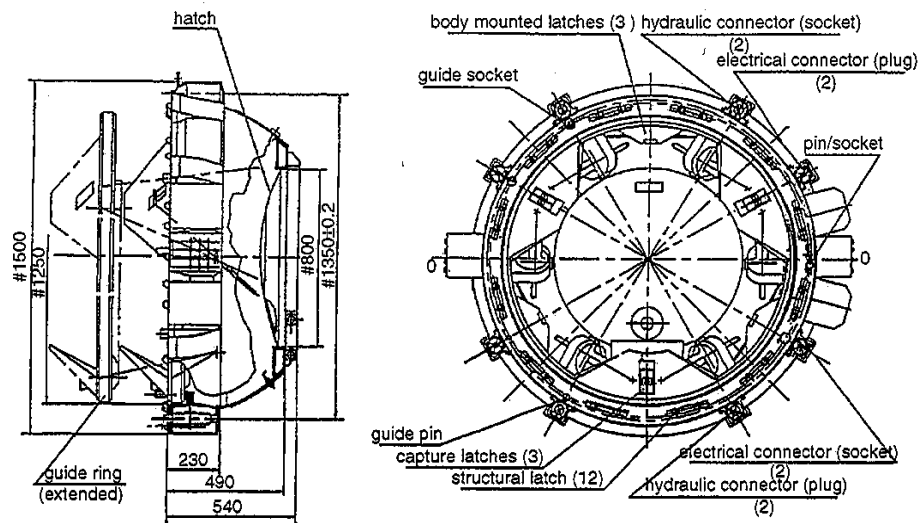
Figure 16: APDS docking system (Fehse, 2003)

NASA Low Impact Docking Mechanism

A team of NASA engineers, with support from Lockheed Martin engineers,
developed the NASA Low Impact Docking Mechanism (LIDM) for the X-38 to dock with
the ISS. With the cancellation of the X-38, the LIDM was modified for the Orion capsule.
There are a few features of this docking system that makes it unique. The first is that is
force sensor driven. It has a closed loop controlled electro-mechanical alignment and

attenuation system with linear actuators (Fehse, 2003). It also has an electro-magnetic

latch system.
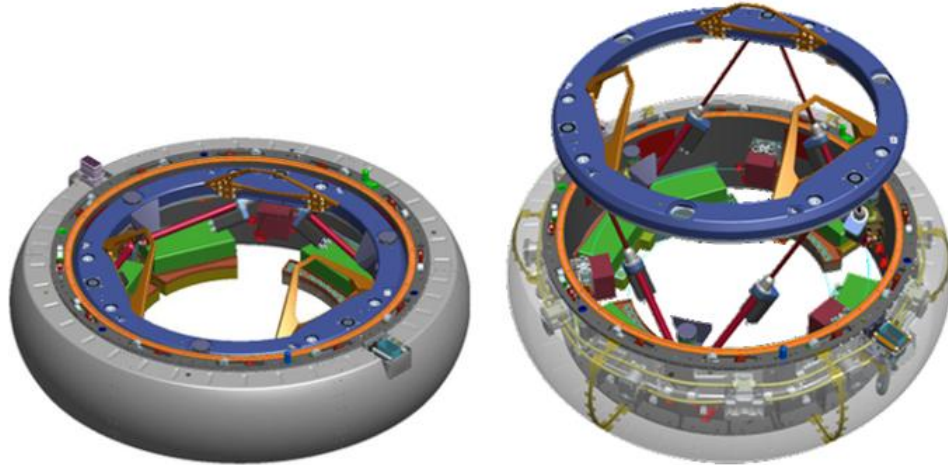
Figure 17: NASA Low Impact Docking Mechanism from

http://en.wikipedia.org/wiki/File:Passive_and_active_NDS..png

Figure 17 shows the LIDM closed on the left and extended on the right.

"All previous docking mechanisms have required the use of impacts (i.e. velocity or post-

contact thrusting) to create the energy required for soft capture mechanism interface

alignment and capture between mating docking interfaces. Low Impact technology can

be used to greatly reduce and even eliminate the need for impact energy and provide the

flexibility for future mission planners, " (Cook, Aksamentov, Hoffman, & Bruner, 2011).

When contact occurs, the six force sensors that are arranged at 45 degrees with

respect to the contact ring, the same way the linear actuators are arranged, determine

the magnitude and direction of the force vector and the point of force application

(Fehse, 2003).   The linear actuators work to align the contact ring with the contact ring

on the target by the use of the closed loop control system that moves the linear

actuators until the forces that the sensors pick up are balanced. Next, the three

electromagnets turn on to latch the contact ring of the target to the contact ring of the

chaser (Fehse, 2003). The control software uses the linear actuators to dampen the

impact of the chaser to the target.   Finally, the linear actuators bring in the chaser to

the target by retracting themselves.

International Docking System Standard (IDSS)

In 2008 NASA and its international partners in the International Space Station

(ISS) worked to come up with a common mechanism design for joint operations

between countries in space. NASA wanted its Low Impact Docking System (LIDS),

another name for the LIDM, docking system to be the standard for the ISS. At the end of

negotiations in 2010, a compromise of the hard capture system based on the APAS and

the soft capture system based on the LIDS would be combined to create a new common

mechanism (Cook, Aksamentov, Hoffman, & Bruner, 2011). This common mechanism

would allow joint missions between countries to low Earth orbit and exploration

beyond.

The resulting document from this was the International Docking System

Standard Interface Definition Document (IDSS IDD). This document does not specify

exact interface requirements but it provides enough information for countries to

independently perform all of the design and analysis to create a docking system that is

able to mate with the docking interface (Cook, Aksamentov, Hoffman, & Bruner, 2011).

Dynamics of Contact and Capture

The movement of the chaser and target spacecraft can be derived from the momentum law. For translational motion over the time period $\Delta t = t_1 - t_0$, the relation between the change of velocity vector ΔV and the force F on a body with mass m is Equation 1 (Fehse, 2003).

Equation 1

$$\int_{t_0}^{t_1} F dt = m \cdot \Delta V$$

If the point of impact is not located on a line connecting the two centers of mass of the target and the chaser then the change of angular momentum must also be taken into account, thus Equation 2.

Equation 2

$$I \cdot \Delta \omega = \int_{t_0}^{t_1} (r \times F) dt$$

In Equation 2 $\Delta \omega$ is the change of angular velocity of the body during the time period Δt, I is the inertia tensor of the body, and r is the distance vector between the contact point and the center of mass of body b. For the rest of this section, the target will be referred as body b and the chaser will be body a.

For a central impact where the chaser will have first contact with the target along the line of their center of mass, along of one of the main axes such as the x-axis, this is a simplified case. This makes Equation 1 become Equation 3.

Equation 3

$$\int_{t_0}^{t_1} F_x(t)\, dt = m \Delta V_x$$

The target and the chaser have masses m_b and m_a respectfully, and velocities in the x-direction $V_a(t)$ and $V_B(t)$, the changes of velocity due to impact are:

Equation 4

$$m_a(V_{a1} - V_{a0}) = -\int_{t_0}^{t_1} F_x\, dt$$

Equation 5

$$m_b(V_{b1} - V_{b0}) = -\int_{t_0}^{t_1} F_x\, dt$$

Where V_{a0} is the velocity of the chaser at contact; t_0 is time at contact; t_1 is any time before the target and chaser separate again.

Impact can be broken down into two parts: the compression phase and the expansion phase. At the end of the compression phase, when the target and chaser have assumed the closest distance, they have the same velocity (Fehse, 2003). This is also the case if capture takes place, the two will move with a common velocity V_c. V_c can be solved for because at the end of the compression phase the forces acting on the target and chaser are equal in magnitude but opposite in direction, so for the case of a central impact:

Equation 6

$$m_b(V_c - V_{b0}) = -m_a(V_c - V_{a0})$$

Equation 7

$$V_c = \frac{m_a V_{a0} + m_b V_{b0}}{m_a + m_b}$$

If capture fails, the spring forces of the spring-damper system of the docking/berthing system will push the two spacecraft away from one another (Fehse, 2003).

For a non-central impact, assume an impact of body a on body b with a velocity of V_a in the x-direction, where on body a the force line passes through the center of mass, but on body b a distance r exists in the y- or z- direction between the line of impact and the center of mass (Fehse, 2003). Also assume that r will not change during Δt, the angular momentum using Equation 2 becomes:

Equation 8

$$I_b \cdot (\omega_{b1} - \omega_{b0}) = r \int_{t_0}^{t_1} F_x(t) dt$$

To simplify this further, assume V_{b0} and ω_{b0} both are equal to zero. At the end of the compression phase both bodies have the same velocities, where on body b the velocity is the sum of a translation of the center of mass and of a translation of the impact point due to the induced angular velocity about the center of mass:

Equation 9

$$V_c = V_{a1} = V_{b1} + r \cdot \omega_{b1}$$

The momentum equation for body a is still Equation 4, but for body b Equation 5 and Equation 8 have to be considered for the momentum exchange. When the initial

39

conditions that were assumed earlier, V_{b0} and ω_{b0} both are equal to zero, Equation 5

and Equation 8 become:

Equation 10

$$m_b V_{b1} = \int_{t_0}^{t_1} F_x dt$$

Equation 11

$$\frac{I_b}{r} \omega_{b1} = \int_{t_0}^{t_1} F_x \, dt$$

Combining Equation 4, Equation 8, Equation 10, Equation 11, and solving for V_{b1}

Equation 12 can be found that will describe the translational motion of body b:

Equation 12

$$V_{b1} = V_{a0} \frac{I_b \cdot m_a}{I_b(m_b + m_a) - r^2 m_a m_b}$$

Angular motion is found to be:

Equation 13

$$\omega_{b1} = V_{a0} \frac{r \cdot m_a \cdot m_b}{I_b(m_b + m_a) - r^2 m_a m_b}$$

This is a basic understanding of contact and capture process. In a real case, the

impact will not be along one of the main axes or go through the center of mass (Fehse,

2003). To calculate the impact forces and the dynamic reactions of two spacecraft, the

exact impact point and the angles of impact with respect to the body coordinates of the

two spacecraft will have to be determined before any further analysis can be started

(Fehse, 2003). These angles and exact point of contact depend on the geometry of the

spacecraft, docking interfaces of the spacecraft and state vectors of the spacecraft.   In

the simulation part of this paper it will be discussed in more detail.

Shock attenuation dynamics

When two bodies impact there are elastic and/or plastic deformations

depending on material properties. This is no different in space. With space docking and

berthing operations, one goal is to minimize elastic and plastic deformations. To reduce

contact forces and increase the time to allow for capture, some type of shock absorbing

system is needed. This will help prevent any major elastic or plastic deformation. The

shock absorbing system is designed to increase the amount of travel after contact due

to elastic and plastic deformation and to absorb a part of the kinetic energy by viscous

damping and/or friction (Fehse, 2003).
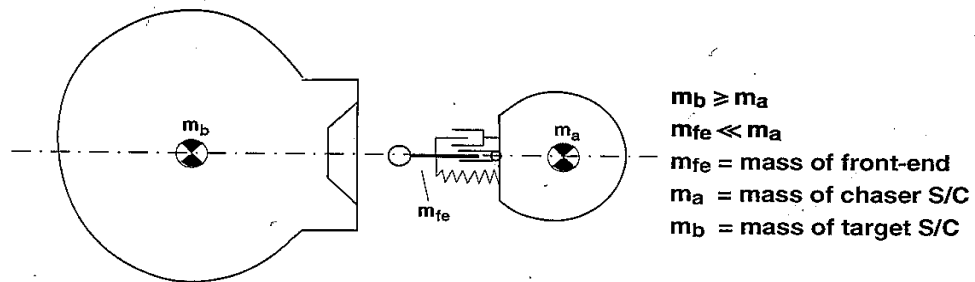
Figure 18: Simplified model of a central impact with spring-damper system (Fehse, 2003)

Figure 18 shows a simplified model of a central impact with a spring-damper

system. Shock attenuation systems usually consist of elastic elements such as springs

that convert kinetic energy from the motion of the spacecraft into heat. "The mass of

the shock absorber system is assumed to be very small compared with the masses of

each of the vehicles," (Fehse, 2003). Dampers are energy converting functions that can be implemented either as a velocity dependent friction device, or as a constant friction device, or a combination of the two.   Viscous dampers are an example of a velocity dependent friction device. Viscous dampers are a fluid that is pressed through a small gap and the resistance force depends on the speed of the fluid going through the gap. Another type of velocity dependent friction device is an eddy current damper. An eddy current damper is a damper whose resistance torque is dependent on the angular velocity of a metal disc rotating in a magnetic field.

The equation of motion of a mass connected with a spring and velocity proportional damper to a fixed point in an internal frame is:

Equation 14

$$F_x(t) = m\ddot{x} = -D\dot{x} - Cx \pm F_f$$

Where D is the damping constant, C is the spring constant and F_f is the constant friction force and the sign of the friction force is always opposite to the direction of motion (Fehse, 2003).

In the case where there are two masses, m_a and m_b, are connected by a spring and viscous damper system that is shown in Figure 18. The equation of motion for body a is:

Equation 15

$$m_a\ddot{x}_a = -D\Delta\dot{x} - C\Delta x$$

The equation for body b is:

Equation 16

$$m_b \ddot{x}_b = -D\Delta\dot{x} - C\Delta x$$

Where Δx = x₁ − x₀ is the distance and $\Delta\dot{x} = \dot{x}_1 - \dot{x}_0$ is the relative velocity

between the two bodies. Combining and subtracting Equation 15 and Equation 16 from

each other, Equation 17 is found:

Equation 17

$$\Delta\ddot{x} = \ddot{x}_1 - \ddot{x}_0 = -(D\Delta\dot{x} + C\Delta x)\left(\frac{1}{m_a} + \frac{1}{m_b}\right)$$

This can be rewritten and simplified to:

Equation 18

$$\Delta\ddot{x} = -(D\Delta\dot{x} + C\Delta x)\frac{1}{m_e}$$

This equation can be shown as a diagram in Figure 19 below:
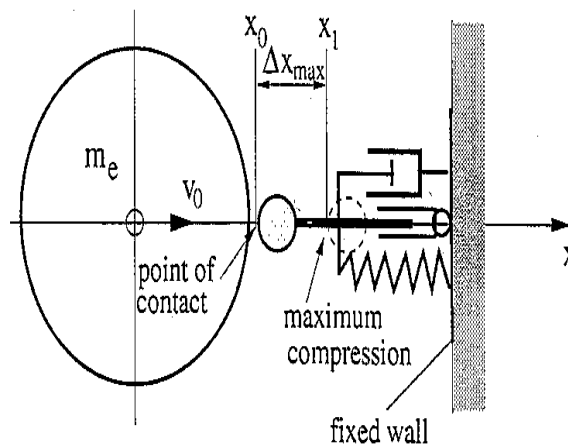
Figure 19: Simplified equivalent mass model for central impact (Fehse, 2003)

43

Figure 19 is a simplified spring-damper model with an equivalent mass. The advantage of this definition is that only the relative motions between the two masses need to be considered. This definition of an equivalent mass is also valid for a constant friction damper system (Fehse, 2003). Equation 14 shows that there are many ways to reduce kinetic energy including using a spring, using a solid braking system, using a velocity proportional braking system, or by any combination of these functions.

Shock attenuation by spring only

The equation of motion for this case is:

Equation 19

$$m_e \ddot{x} = -Cx$$

Shock attenuation by spring only

The equation of motion for this case is:

Equation 20

$$m_e \ddot{x} = -Cx$$

The solution of this differential equation is:

Equation 21

$$x(t) = c_1 \cos \omega_1 t + c_2 \sin \omega_1 t$$

The $\omega_1 = \sqrt{\dfrac{C}{m_e}}$ is the resonant frequency. The constants can be obtained from the boundary conditions for t_0:

Equation 22

$$c_1 = x_0; \, c_2 = \frac{v_0}{\omega_1}$$

Damping by solid friction braking only

For this case the equation of motion is:

Equation 23

$$m_e \ddot{x} = \pm F_f$$

The direction of the friction force is always the opposite of the direction of velocity. The solution for the travel over time can be found by double integration:

Equation 24

$$x(t) - x_0 = \Delta x(t) = \left(v_0 \pm \frac{F_f}{2m_e} t \right) t$$

The time is valid up to the time where dx/dt becomes zero.

Damping by velocity proportional braking only

For this case the equation of motion is:

Equation 25

$$m_e \ddot{x} = -D\dot{x}$$

After integrating this equation once, the solution for travel over time can be found. Using the homogenous solution $(y = c \cdot)$ of a first order linear differential

equation($\int dt$)($\dot{y} + py = 0$). With substitutions $D/m_e x(t) - c_1 = y$ and$D/m_e = p$,

the equation becomes:

Equation 26

$$x(t) - x_0 = \Delta x(t) = -\frac{m_e}{D} v_0 \left(e^{-\frac{D}{m_e}t} - 1 \right)$$

Combination of a velocity proportional braking device and spring

For this case the equation of motion is:

Equation 27

$$F_x(t) = m\ddot{x} = -D\dot{x} - Cx$$

There are solutions of Equation 27 if is written in this form of a differential

equation:

Equation 28

$$\ddot{x} + 2\delta\dot{x} + \omega_1^2 x = 0$$

Where the coefficients are $\omega_1^2 = C/m$ and$2\partial = D/m$. The constant ω_1 is the

resonant frequency of the spring-mass systems. The solutions are the following

equations:

Equation 29

$$x(t) = e^{-\delta t}(k_1 \cos \gamma t + k_2 \sin \gamma t) \; for \; \gamma^2 = \omega_1^2 - \delta^2 > 0$$

Equation 30

$$x(t) = e^{-\delta t}(k_1 \cos h\gamma t + k_2 \sin h\gamma t) \; for \; \gamma^2 = \omega_2^1 - \delta^2 < 0$$

Equation 31

$$x(t) = e^{-\delta t}(k_1 \cos h\gamma t + k_2 \sin h\gamma t) \; for \; \gamma^2 = \omega_1^2 - \delta^2 = 0$$

Equation 29 is a case of an oscillation with low damping. Equation 30 is a case of

an oscillation with high damping. Equation 31 is a boundary case of oscillation with

aperiodic damping. Equation 31 is the ideal when $\omega_2^1 = \delta^2$ case for avoidance of

oscillations. This ideal case will never happen in real operations, but it is useful as a

reference for the assessment of spring-mass damper systems (Fehse, 2003). This case

leads to simple math expressions that can be solved quickly. This means that the

constants k_1 and k_2 can be solved from the boundary conditions to be $k_1 = x_0$ and

$k_2 = v_0 + \delta x_0$ where Δx_0 and v_0 are the conditions at the start of motion. Using these

constants that were just defined and using Equation 17, Equation 18 along with

Equation 31 which is the equation for relative position of Δx, the relative velocity

$v = \Delta \dot{x}$, relative acceleration $\Delta \ddot{x}$ between the two bodies after contact become:

Equation 32

$$\Delta x(t) = e^{-\delta t}[\Delta x_0 + (v_0 + \delta \Delta x_0)t]$$

Equation 33

$$\Delta \dot{x}(t) = e^{-\delta t}[v_0 - (v_0 + \delta \Delta x_0)\delta t]$$

Equation 34

$$\Delta \ddot{x}(t) = \delta e^{-\delta t}[(v_0 + \delta \Delta x_0)\delta t - 2v_0 - \delta \Delta x_0]$$

In this application of a spring-mass damper system Δx_0 is zero, since the system is at a neutral position at the instant of contact. The definition of the factor δ for the aperiodic case in Equation 31 is:

Equation 35

$$\delta = \omega_1 = \sqrt{\frac{C}{m_e}}$$

Using Equation 32, Equation 33, and Equation 34, the relative motion and force over time between two bodies can be calculated. The central impact case calls for the forces acting between two bodies that are defined by Equation 27 and the definition of the equivalent mass creates Equation 36:

Equation 36

$$F_x(t) = m_e \Delta \ddot{x}$$

Shock attenuation systems for central docking systems

The active end of a central docking system is the rod attached to the chaser. Two main forces will occur at contact: a longitudinal force along the rod axis, and a lateral force that causes torque about the connection point at the base of the rod to the chaser. The longitudinal force is a compression force that is along the rod axis. The rod also has an angular motion about a spherical bearing at its base due to this compression force. To dampen this longitudinal force, one of the damper types that have been discussed earlier will have to be applied. Figure 20 shows a central docking system that will rebound with and without a spring-damper system.
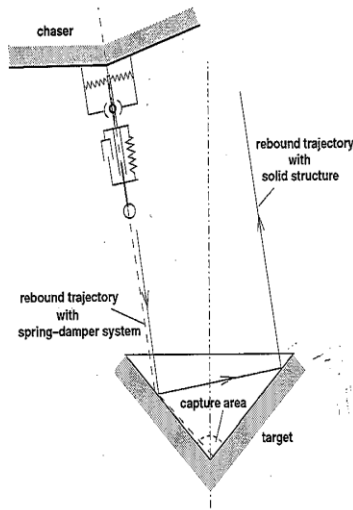
Figure 20: Central docking system rebound with and without spring-damper (Fehse, 2003)

If the rod does not have any flexibility, mainly in the lateral direction, the tip of

the rod will not move to the center of the cone where the capture area is (Fehse, 2003)

Equation 24 and Equation 26 show that motion attenuation in a longitudinal direction

does not require the usage of springs. For capture it can be better sometimes to have

only a velocity proportional braking system during the initial part of motion. "A spring

system could push the capture interfaces after maximum excursion, if the system was

not properly tuned for aperiodic damping," (Fehse, 2003). Springs when stretched to

their maximum could interfere with the mechanism of capture between the target and

chaser if it is not designed properly.

Shock attenuation systems for peripheral docking systems

In peripheral docking systems a complex system is required for shock

attenuation and alignment for capture. The reason it is so much more complicated for

peripheral docking systems to capture then a central docking system, is that a

peripheral docking system with any damping will act just like a quarter that is dropped face flat onto a table (Fehse, 2003). Anyone who has played with coins like this will know that the coin never impacts with the table the same way twice. With central docking systems, it is more like a ball being dropped on the table, as long as it is dropped the same it will bounce the same. A six degree of freedom damping system is needed to deal with the contact conditions that include lateral velocities, linear and angular misalignments, angular velocities, and velocity along the nominal approach axis.

There is a common arrangement that is used for this purpose; it is called a Stewart platform as shown in Figure 21.
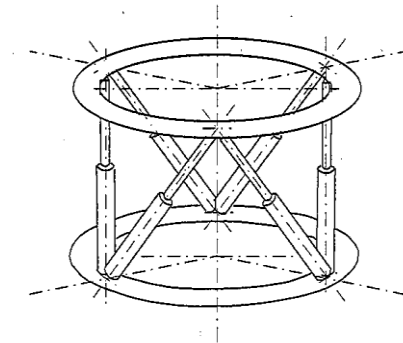
Figure 21: Stewart platform arrangement (Fehse, 2003)

The Stewart platform is an arrangement of six linear motion elements, connected to three points each on the upper and lower rings as shown in Figure 21. Just to note: the position of the connecting points between the two rings are shifted by 60 degrees.

Another reason that makes it much more complicated to design a damping system for a peripheral docking system is the use of passive latches to achieve capture.

This means that capture will only happen once the two contact rings are aligned with very small margin of error, which means that the system needs to be fully damped out (Fehse, 2003). For a central docking system the flexible rod can just be pushed into the capture hole at the center of the reception cone and it will be locked in place.

Passive latches have a short coming that they cannot adjust for misalignments ad require a very small margin of error. An action system on the other hand is able to adjust to misalignments, to align the two contact rings to mate. The linear actuators that are the damping system can be used to align the contact ring. The best example of this being used is the NASA Low Impact Docking System or NASA Low Impact Docking Mechanism that has been discussed earlier.

Velocity proportional viscous damper

A velocity proportional viscous damper is most commonly a combination of spring and hydraulic damper system. The best example of this is the shock absorbers for cars. In one Earth gravity application it is a piston in a cylinder where the gap between the piston and the wall is the flow restrictor. In space the piston design is not as effective as it is on the ground. In space applications the design is an arrangement of two bellows, connected by an orifice that acts as the flow restrictor (Fehse, 2003). One problem with the bellow setup is that the ratio of extended to compressed length is relatively small.

Velocity proportional eddy current damper

The velocity proportional eddy current damper uses the physical effect that when eddy currents are applied to a piece of metal when that metal is moved in a magnetic field. These eddy currents interact with the magnetic field that causes the energy to be dissipated. This creates a magnetic drag force proportional to the velocity. This magnetic drag force slows down the motion of the piece of metal (Fehse, 2003). To create a high damping effect, the translational motion is converted into a rotation by a screw type of motion converter that drives a metal disc that moves through the gap of a permanent magnet. This type of damping system was used on the Soyuz/Progress probe-drogue docking system.

Friction Damper

In most mechanisms there is some type of friction damper; it can be caused by the sliding or rolling friction in bearings. Friction dampers can be applied when its force is proportional to a compression force, such as by moving a disc between two others which are compressed by spring pre-load (Fehse, 2003). The translational motion can be converted into a rotation, and this allows the amount of friction in a friction brake to be adjusted by spring pre-loading.

Actively controlled motion damping

Another type of damping system is actively controlled motion damping. This is used on the NASA Low Impact Docking System or NASA Low Impact Docking

Mechanism. This is the most complex of all the damping systems discussed in this paper. "In this system, the force vector and its application point is actively sensed by six load cells at the circumference of the contact ring, and damping and alignment is provided by motion control of the six linear actuators arranged in a Stewart platform configuration," (Fehse, 2003). A closed loop controlled electro-mechanical system that is comprised of force sensors, controller and linear actuators, allows for a large range of damping characteristics that can be changed by the control software.

Capture Strategies

There are two types of capture strategies: after first contact and before first contact. The after contact strategy is once first contact occurs, capture operations are initiated between the target and chaser (Fehse, 2003). This case is docking operations. Capture before first contact requires a sensor function which identifies the entry of the capture interfaces into the capture range. This is berthing operations.

Types of Capture

There are five main types of capture: central docking systems, passive capture latch for peripheral systems, active capture latch for peripheral systems, magnetic capture devices, and capture mechanism for berthing, also known as grappling.

Central docking systems use a docking method known as impact docking. It uses the strategy of capture after first contact: contact will happen on a point on the surface of the reception cone that will guide the tip of the rod into the capture hole in the

center of the reception cone (Fehse, 2003). Spring-loaded latches arranged on the tip of the rod engage with the corresponding catches in the hole in the reception cone to create capture as discussed earlier in this paper.

Passive capture latch for peripheral systems are designed to be used for capture before and after contact. Passive capture latches are spring-loaded and mounted in the center of the petals to engage with corresponding catches on petals of the opposite docking ring (Fehse, 2003).   To have this happen, a relatively high contact velocity is required for successful capture.

Active capture latch for peripheral systems are different then the passive latch because it requires operation of an electro-motor. The capture before contact strategy needs to be applied here to allow enough time for closure of all the latches (Fehse, 2003). This only works if the approach velocity is small compared with the latch closure velocity. The final alignment requirements at instant of capture will be less than for passive capture latches, which make this type more reliable (Fehse, 2003). The downside of this is that larger misalignments at the entrance into the reception range would have to be compensated for by large dimensions of the capture latches.

Magnetic capture devices are comprised of a number of electro-magnets arranged on the circumference of the contact ring. When the contact rings are brought close together they will attract each other ensuring contact and alignment (Fehse, 2003). The advantages of this system are that there is no need for mechanical capture latches and alignment occurs automatically. The disadvantages of this system are that

with the application of a magnetic device for docking that the force characteristics of

magnets decrease over distance. This means a magnet may not be strong enough to

pull in the spacecraft at a longer distance. As the chaser and target get closer together

their velocity toward one another will increase (Fehse, 2003). This problem can be

overcome by actively controlling the magnetic forces as a function of distance or by

actively aligning the contact rings with respect to each other and engaging the electro-

magnets only when the contact rings are close to one another.

There is a special capture mechanism for berthing during the grappling/ grasping

phase of the operation. The most common design in use is the end-effector developed

by the Canadian Space Agency (CSA) together with the manipulator arm for the US

Space Shuttle and now used on the ISS (Fehse, 2003).   This can be seen in Figure 22

below.
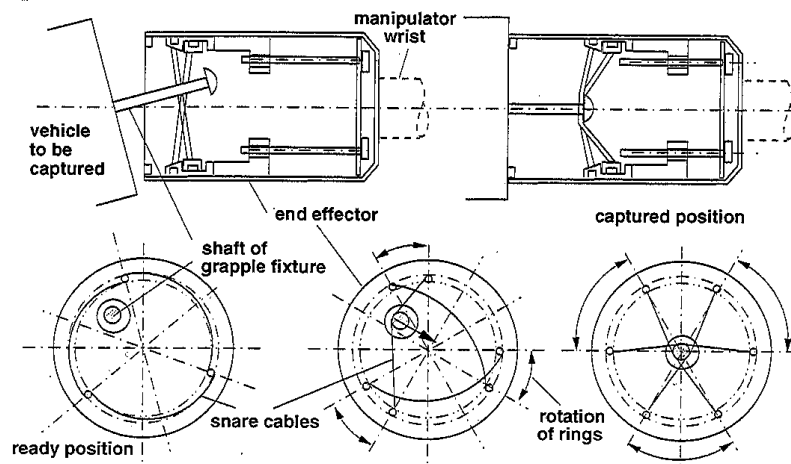
Figure 22: Manipulator end-effector and grapple fixture developed by CSA (Fehse, 2003)

Simulations of a peripheral docking system

Before the construction of a test-bed for the transfer system between the ILH and PER, some docking simulations must be complete. This is to allow an understanding of the forces involved in a docking process. Work in this field has been done with semi-physical simulation at the Harbin Institute of Technology in Harbin, China. The test procedure they used for a peripheral docking system is restated below (Yang, Hao, & Qiu-sheng, 2007):
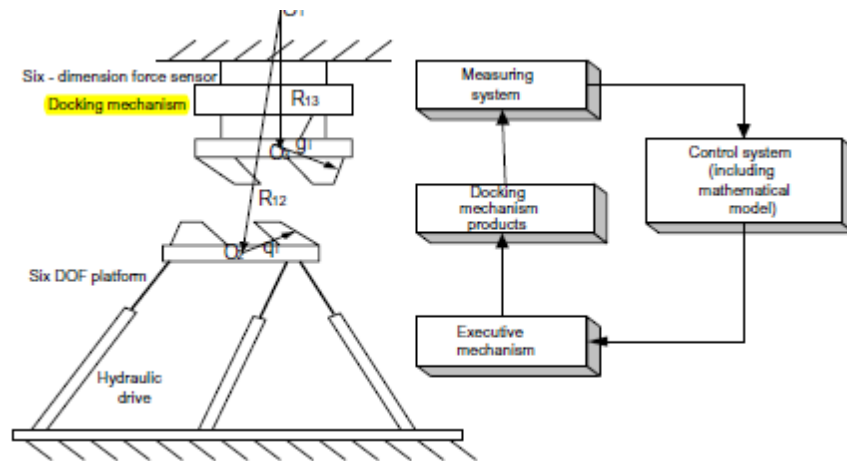
Figure 23: Semi-physical simulation platform (Yang, Hao, & Qiu-sheng, 2007)

Table 3: Steps for Test Procedure for peripheral docking system

Step	
1	Relative motions between target and chaser are determined by the relative motion of the two spacecraft to their initial position
2	The motions of the spacecraft are defined in a six degree of freedom coordinate system that is translated to the movement of the test platforms that are acting as the chaser and target spacecraft
3	After impact, force sensors on the contact rings report the forces and torques
4	The control system accepts the information from the force sensors and reacts to the forces by active and passive means
5	Motion variations of the chaser and target are computed by a mathematical model at the same time as the Control system reacts to the forces
6	Relative motions of the chaser and target spacecraft are recorded
7	Relative motions are realized by chaser spacecraft

Steps 3-7 are repeated until capture is recorded. To sum up this docking procedure: the control system measures the docking forces then computes the relative motions according to a pre-determined mathematical model, then the control system of the chaser uses this data to realign itself to be in a position to achieve capture (Yang, Hao, & Qiu-sheng, 2007). The mathematic model is based on the same dynamics that are discussed earlier in this thesis; in the docking dynamics section. Using this semi-physical testing process the docking impact dynamic model can be further defined.

It is necessary to describe the motion of the docking mechanism and compute the impacting force when the chaser impacts the target. During the impacting phase the vector relationship of the forces is shown in Figure 24.
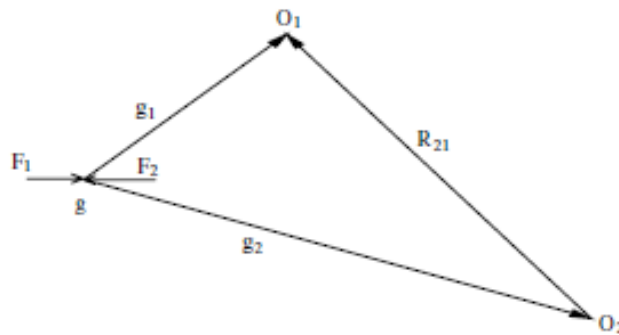
Figure 24: Vector relationship of impacting forces (Yang, Hao, & Qiu-sheng, 2007)

O_1 is the center of mass of the chaser; O_2 is the center of mass of the target (Yang, Hao, & Qiu-sheng, 2007). Following this model, the dynamic model of impact follows:

Equation 37

$$m_3 \ddot{R}_{13} = F_h - \sum_{i=1}^{m} F_i$$

Equation 38

$$J_3 \cdot \dot{\omega}_{13} + J_3 \cdot \widetilde{\omega_{13}} \cdot \omega_{13} = A_{31} M_h - \sum_{i=1}^{m} \tilde{g}_i \cdot A_{31} F_i$$

Where:

$\ddot{R}_{13}, \omega_{13}$ are the acceleration and, angle velocity of the guiding petal of the capture system relative to the chaser respectively.

A$_{31}$ is the conversion matrix from the coordinate 1 of the chaser to the coordinate 3 of the guiding petal.

F$_i$ is the impacting force of the ith impacting point

F$_h$,M$_h$ is the bumping force and torque that the guiding petal supports

G$_i$ is the position vector of the impacting point on the guiding petal

M is the number of impacting points

The equations above are when the guiding petal is not closed (Yang, Hao, & Qiu-sheng, 2007). Considering the geometry relation of the impacting point shown in Figure 24, m, the number of the impacting points, geometry constraint equations become (Yang, Hao, & Qiu-sheng, 2007):

Equation 39

$$\overrightarrow{R_{12}} + \overrightarrow{q_i} - \overrightarrow{R_{13}} - \overrightarrow{g_i} = 0$$

To determine the passive impacting force of the two spacecraft, there is another approach. Where g is the impact point; F_1, F_2, are the impacting forces of the chaser and target respectively, g_1, g_2, are the radius vectors; O_1, O_2, are the original point of the chaser and target coordinates (Yang, Hao, & Qiu-sheng, 2007). The torque acting on the chaser is:

Equation 40

$$\overrightarrow{M_1} = \overrightarrow{F_1} \times \overrightarrow{g_1}$$

The torque acting on the target is:

Equation 41

$$\overrightarrow{M_2} = \overrightarrow{F_2} \times \overrightarrow{g_2}$$

Using Figure 24:

Equation 42

$$\overrightarrow{R_{21}} = \overrightarrow{g_1} - \overrightarrow{g_2}$$

Adding up Equation 40 and Equation 41 along with the vector relationship, the relationship of the force, and the counter force of $\overrightarrow{F_1}, \overrightarrow{F_2}$ is Equation 43 (Yang, Hao, & Qiu-sheng, 2007).

Equation 43

$$\overrightarrow{M_2} = \overrightarrow{F_1} \times \overrightarrow{R_{21}} - \overrightarrow{M_1}$$

To sum this up, according to the relationship of the force and counterforce, the impact force that the target supports can be determined by the impact force of the chaser, and the impact torque can be determined by Equation 43 (Yang, Hao, & Qiu-sheng, 2007).

Simulations for Central Docking Systems

The pin-cone docking system, also known as the probe-drogue system since its development in the 1960s to 1970s, has been used over 230 times in successful spacecraft docking operations. At the development stage in the 1960s-1970s there was no way to analyze the dynamics of the system in great detail due to insufficient computer power and the absence of algorithms for modeling the mechanical systems of solid bodies (Yaskevich, 2006). The lack of computing power in the 1960-1970s limited the ability to create a complete dynamic analysis in great detail for central docking systems. In the year 2000 the EADS Company working with the European Space Agency (ESA) developed, as part of the European ATV transport spacecraft to the International Space Station (ISS), complete mathematical models of the dynamics of this docking operation (Yaskevich, 2006).

Differential equations of motion are considered which take into account the elasticity of spacecraft constructions and all basic peculiarities of kinematics of a docking mechanism, to develop a model of central docking operations. The first thing needed is to define a coordinate system to be used in the model of docking, which is show below in Figure 25.
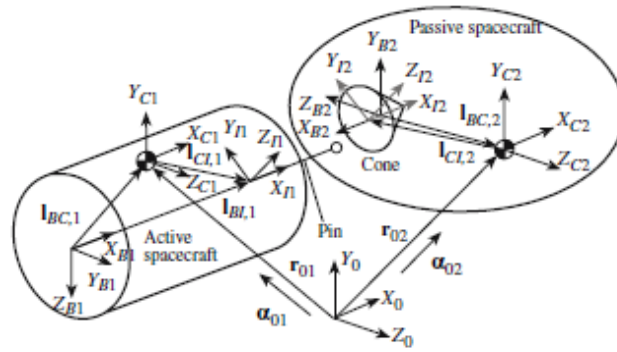
Figure 25: Coordinate system used in the model of docking (Yaskevich, 2006)

The model of docking, based on these detailed differential equations of motion, allows an in-depth analysis of the dynamic process from the moment of first contact of docking spacecraft until last stage of capture while accounting for different modes of operation of spacecraft control systems (Yaskevich, 2006). This model views each impact of docking as a process in time, rather than as an instantaneous change of velocities of the spacecrafts (Yaskevich, 2006). Contact imposes on the motion of a spacecraft an uncontrolled constraint which is shown by the corresponding reaction force. The model determines these reaction forces by parameters of rigidity and damping that depend on the type of contact of the docking mechanisms (Yaskevich, 2006). The earlier section of dynamics of docking and berthing operations explains the basic equations of motion that this model is based on in its simplest form.

Figure 26 shows the computing scheme for the docking mechanism for the model. On the right side of the figure is the chaser with the probe of the central docking system attached to the shock attenuation system. The center box shows the axial damper of the docking mechanism, where the screw-nut of a ball-screw gearing (BSG) is converted into rotation of a

spring mechanism (SM) with a friction brake (FB) and electromagnetic brake (EMB). The box to

the left is when the head of the probe impacts with the wall of the drogue. The model uses the

differential equations of motion for each of the dampers, and parameters of the spacecraft of

rigidity to define a series of equations for each moment of time during the docking process.
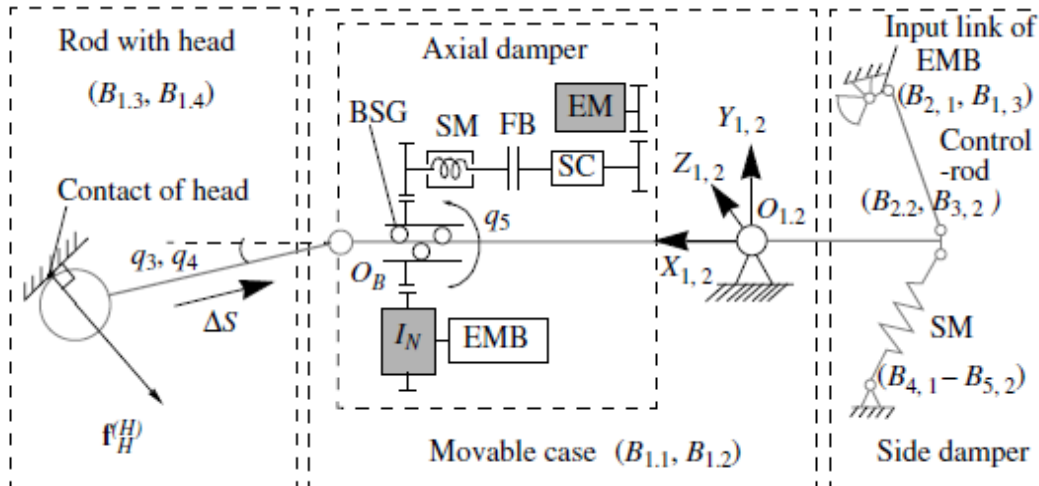
Figure 26: Computing scheme for docking mechanism (Yaskevich, 2006)

The detailed description of dynamics of the model is beyond the scope of this paper,

because of the complex algorithms used, and requirements of complicated mathematical

modeling. The paper "Combined Equations of Motion for Description of Dynamics of

Spacecraft Docking Using the Pin and Cone System" by A.V. Yaskevich, which is cited in this

thesis, explains the detailed process of developing the working model of the dynamics of a

central docking system.

Simulation for Berthing Operations

Impact between the chaser and target happens in both the cases of docking and

berthing. In berthing, the impact is more controlled than in docking operations. The nature of

impact and post-impact dynamics depend on whether the berthing/docking is successful or if

there is a rebound (Xavier, Sun-Wook, Michel, Arun, & Gilbert, 1995). At McGill University in

Montreal, Canada, a team worked to study post-impact dynamics associated with manipulator-

assisted docking/berthing operations (Xavier, Sun-Wook, Michel, Arun, & Gilbert, 1995). Using

Lagrangian formulation for individual bodies and then eliminating the constant forces and

moments with the help of the natural orthogonal complement of the velocity constraint matrix,

the equations of motion for two multi-body systems before and after impact have been defined

(Xavier, Sun-Wook, Michel, Arun, & Gilbert, 1995). This impact model can handle impact from

fully plastic to fully elastic. The mathematics behind the development of the model for berthing

operation simulation is beyond the scope of this thesis, but a summary of what was discovered

will follow. It was found that there is a significant difference in the post-impact motion

between the fully plastic and the fully elastic cases (Xavier, Sun-Wook, Michel, Arun, & Gilbert,

1995).   This should be no surprise because each of these cases is on the opposite extremes of

impact types.

In the plastic case, the chaser has a large angular momentum, which tends to require

the manipulator arm to extend until singularity configuration of the manipulator arm is

achieved. At this moment, the arm is translated in both the chaser and the base of the target

which causes the chaser to change its direction of rotation and the target to experience

attitude drift (Xavier, Sun-Wook, Michel, Arun, & Gilbert, 1995).

In a non-plastic impact there are differences that depend on the values of two

parameters: friction and energy-loss. The friction parameter is where "impulse that is involved

in the collision at the contact point can be divided into two components; one is along the line of impact (normal impulse) and the other is perpendicular to it (friction impulse)," (Xavier, Sun-Wook, Michel, Arun, & Gilbert, 1995). The post-impact motion of the target-chaser system is influenced by this change in direction and magnitude of the resultant impulse. Energy-loss parameter is where "for a fixed friction parameter, the energy-loss parameter influences the normal impulse so that this parameter also is seen to change the direction and magnitude of the resultant impulse," (Xavier, Sun-Wook, Michel, Arun, & Gilbert, 1995). From this it can be seen that energy-loss and the friction both influence the change in direction and magnitude of the system because they are both used to determine the resultant impulse of the system.

The use of complex mathematics allows the modeling of complicated systems to enable a better understanding of what is happening. With the help of computer modeling, calculations that had not been able to be done before can now be attempted. The models used for the simulation of berthing operations are so complex that just to explain these models is outside the scope of this thesis, but applying what the models have discovered and by using simpler models, a realistic simulation of a docking operation can be done.

Sensors for Docking

Sensors are important for docking/berthing systems. Video sensors can allow the operator to see the operation, contact sensors can tell the operator when contact has occurred, and force sensors can tell the force of impact of the contact. Using any one or a combination can allow for the successful capture of a spacecraft.

Video Sensors

Video sensors allow an operator or a control program to use visual data to make the decisions on how to maneuver the spacecraft to achieve capture. A first generation rendezvous sensor, Video Guidance Sensor (VGS) has been developed by Marshall Space Flight Center (MSFC) and used on two space shuttle missions, STS-87 and STS-95 (Roe & Howard, 2003). The lessons learned from these missions and the advances in video and signal processing has lain a groundwork to improve on the VGS. The Advanced Video Guidance Sensor (AVGS) has this flight heritage of the VGS and the improvement of video and signal processing (Roe & Howard, 2003).   Video is a good choice for a docking/berthing sensor because it is a simple method of viewing an entire field-of-view while getting fast updates of the change in data.

The VGS determines the relative positions and attitudes between the target and chaser spacecraft. The VGS uses laser diodes to illuminate retro-reflectors in the target, and it uses a solid state camera to detect the returning laser diodes from the target (Roe & Howard, 2003). A frame grabber and digital signal processor are used to convert the video data into the relative positions and attitudes. When the VGS was tested in space, its performance was "exceptional

with all design goals met," (Roe & Howard, 2003). The sensor was also able to track in different types of orbital lighting conditions.

The AVGS builds on the success of the VGS with the improvement of video and signal processing capabilities. The AVGS is designed to be a replacement for the existing ISS hemispherical reflector assembly (Roe & Howard, 2003).

There are also a number of other video based docking/berthing sensors under development by NASA. The Johnson Space Center (JSC) has their Automatic Targeting and Reflective Alignment Concept (AutoTRAC) Computer Vision System (ACVS), which is a camera based system that uses reflectors on the target vehicle that are illuminated by flashing Light Emitting Diodes (LEDs) on the chaser (Mitchell, et al., 2008). JSC also has the Natural Feature Image Recognition (NFIR) which is a camera based system that does not require reflectors (Mitchell, et al., 2008).   The Jet Propulsion Laboratory's (JPL) Optech Light Detection and Ranging (LIDAR) which is a laser based system that produces range and intensity data.

The ACVS uses a camera and Light Emitting Diodes (LEDs) with a target of mirrors or reflective surfaces to determine a relative state of range, azimuth, elevation, roll, pitch, and yaw (Mitchell, et al., 2008).   A charged-coupled device camera with LED array using a specific target makes up the ACVS. The first video frame is taken with the LEDs turned on, the next video frame is taken with the LEDs turned off. The two frames are then subtracted from each other with the background being eliminated while leaving the bright return from the retro-reflectors. Next, standard image segmentation techniques are used to determine the retro-

reflectors' location in the image (Mitchell, et al., 2008). This gives the location of the target

relative to the chaser.

The NFIR is a camera-based system but, unlike the AVGS or ACVS, it does not require

LEDs or lasers reflecting off a target. The NFIR can use any high contrast feature on the target

spacecraft for computing motion and pose as long as there is a 3D model for the software to

use. 2D images of the approach features are used to compute 3D motion of the target

spacecraft that is used in turn to update the pose of the target spacecraft (Mitchell, et al.,

2008). A kalman filter is used to estimate the position, orientation from the pose and predict

the locations of the features in the image for the next image frame.

The next generation of video sensor building on the success of the VGS and AVGS

sensors is the Next Generation Advanced Video Guidance Sensor (NGAVGS). The NGAVGS uses

two sets of laser diodes, a mirror which the lasers shine through, a camera that images return

from the lasers to, and hardware, software, and firmware that process the returned images

into relative position and attitude data (Howard & Bryan, 2009).   The sensor is designed to

work with a retro-reflective target. The sensor fires the laser which passes through the filters

and captures the image. Once this is done, the sensor fires the second laser and captures a

second image. The second image is subtracted from the first image and the background is

eliminated. The remaining lit pixel data is converted into a set of spots that are compared to

the target pattern. Once a set of spots that match the target is found, the software is able to

compute the relative position and attitude between the sensor and target (Howard & Bryan,

2009).

Laser Rangefinder

Laser rangefinders are useful sensors that have been applied to space docking/berthing operations. Laser rangefinders use a process called triangulation to figure out the distance of the object. The laser rangefinder uses infrared light (IR) (Society of Robots, SENSORS - SHARP IR RANGE FINDER, 2005). The sensor sends out a pulse of light, wavelength of 850 nm +/- 70 nm, which is reflected back by the object of interest. This light pulse returns at an angle that is dependent on the distance the object of interest is from the sensor (Society of Robots, SENSORS - SHARP IR RANGE FINDER, 2005). Using triangulation, knowing the angle the light pulse left the sensor and returned to the sensor, the distance the object of interest is from the sensor can be found. This is shown nicely in Figure 27.
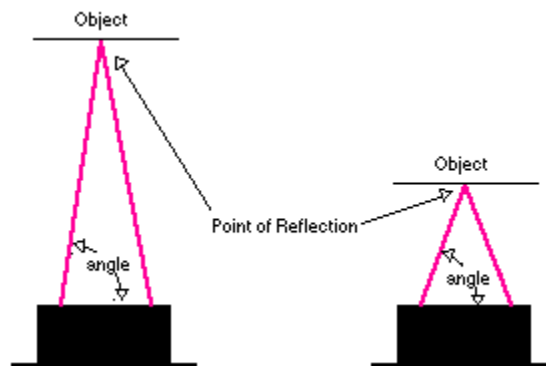
Figure 27: Triangulation from http://www.societyofrobots.com/sensors_sharpirrange.shtml

To do the triangulation, a special precision lens transmits the reflected light to a linear charge-coupled device that is enclosed within the sensor. A charge-coupled device is a group of small light sensitive diodes that converts light particles, called photons, into electrons (Tyson). The diodes are called photosites and the more intense the light is that hits the photosites, the larger the electrical charge, or amount of electrons, will accumulate at that site (Tyson). The

CCD array determines the angle of light pulse that is reflected off of the object of interest. This gives an analog value that can be read by the microcontroller of the laser rangefinder.

One thing to watch out for when working with a laser rangefinder, is the beam width of the laser rangefinder. The rangefinder has a very narrow width, which means that for it to detect the object of interest, it has to be pointing at it (Society of Robots, SENSORS - SHARP IR RANGE FINDER, 2005).

Two Sensor Operations

There has been a study completed at MSFC about using two different types of sensors working as one unit to help with automated rendezvous docking/berthing.   The two different video sensor systems that are being tested working with different laser systems are: the Demonstration of Autonomous Rendezvous Technologies (DART) flight like Serial Number 2 (SN2) and one of the DART final prototypes (FP2) for the tests. Both are flight ready technologies (Howard & Carrington, 2008). The two different lasers systems that were paired with the video sensor systems were commercial laser rangefinders. "The sensor fusion efforts were quite successful in creating a blended solution that was better than anyone sensor's data. Overall, this testing was quite successful," (Howard & Carrington, 2008). This proves that a combination of video and laser sensors is better approach than just a laser or video sensor.

Contact/Force

Contact sensors are useful in docking/berthing operations. The contact sensors can record when impact is made between the two docking interfaces. Contact sensors can be as

basic as a small switch that when pressed completes a circuit to signal contact, or something

that uses the resistance of another object to send the signal. The contact sensors that will be

discussed here will be the basic switch type.
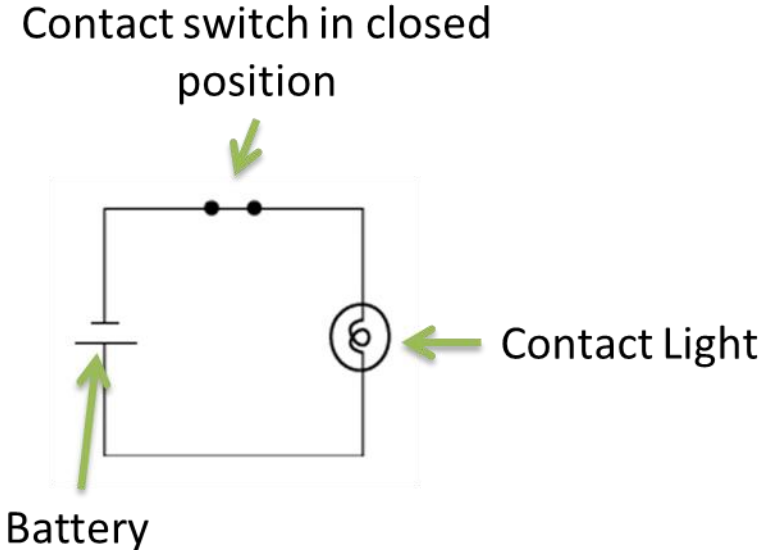
Figure 28: Contact Sensor Circuit

The light switch circuit shown in Figure 28 is an example of a simple switch such as the

kind found in the contact sensors. When the contract sensors are pressed down they make the

throw or the connection between the wires intact and this allows the electricity to go to the

light that will be on the control box.

CHAPTER II
METHODOLOGY

Design

The proposed solution for a transfer system between the ILH and PER is an

extendable pressurized tunnel (EPT). This tunnel will cover a 1 meter, 39.4 inches, gap

between the ILH and PER. It will have a fixed section of .5 meter, 19.7 inches, that will

be mounted to the ILH. This tunnel will have a minimum diameter of 1 meter, 39.4

inches, which is larger than the requirement from NASA for a diameter of .81 meters,

31.2 inches, for one crew member to go through in a space suit in microgravity (NASA,

1995).
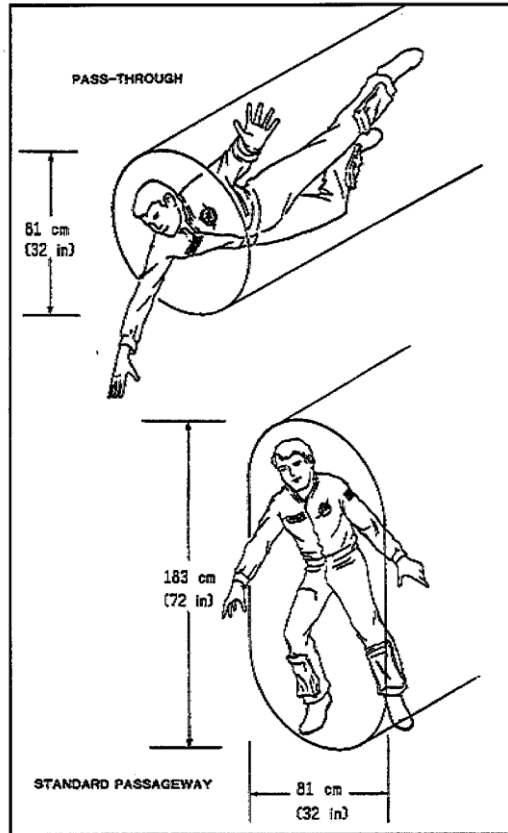
Figure 29: Minimum Translation Path Dimensions for crew travel in microgravity from NASA-STD-3000

Attached to the fixed section of the tunnel will be linear actuators that will control movement in the horizontal direction of a mating ring attached to a cart. The cart will be on a set of rails, and house linear actuators in the vertical direction that will allow vertical movement of the mating ring. This extendable section will go out half a meter and be able to be adjusted to meet different positions of the parked rover. The extendable section of the tunnel will be covered in a bladder to allow it to be pressurized when fully extended using a similar arrangement as the Voskhod spacecraft. In Figure 30 shows the basic idea of the design.

Figure 30: Extendable Pressurized Tunnel shown without the bladder

Structure/Components

There are a number of components that make up the EPT. The first is the fixed section of the tunnel; there are the mating rings, a cart and rail system to allow it to move and a control system to allow adjustment of the tunnel mating rings. In the appendix there is an entire section of the technical drawings for each component and subsystem of the tunnel.
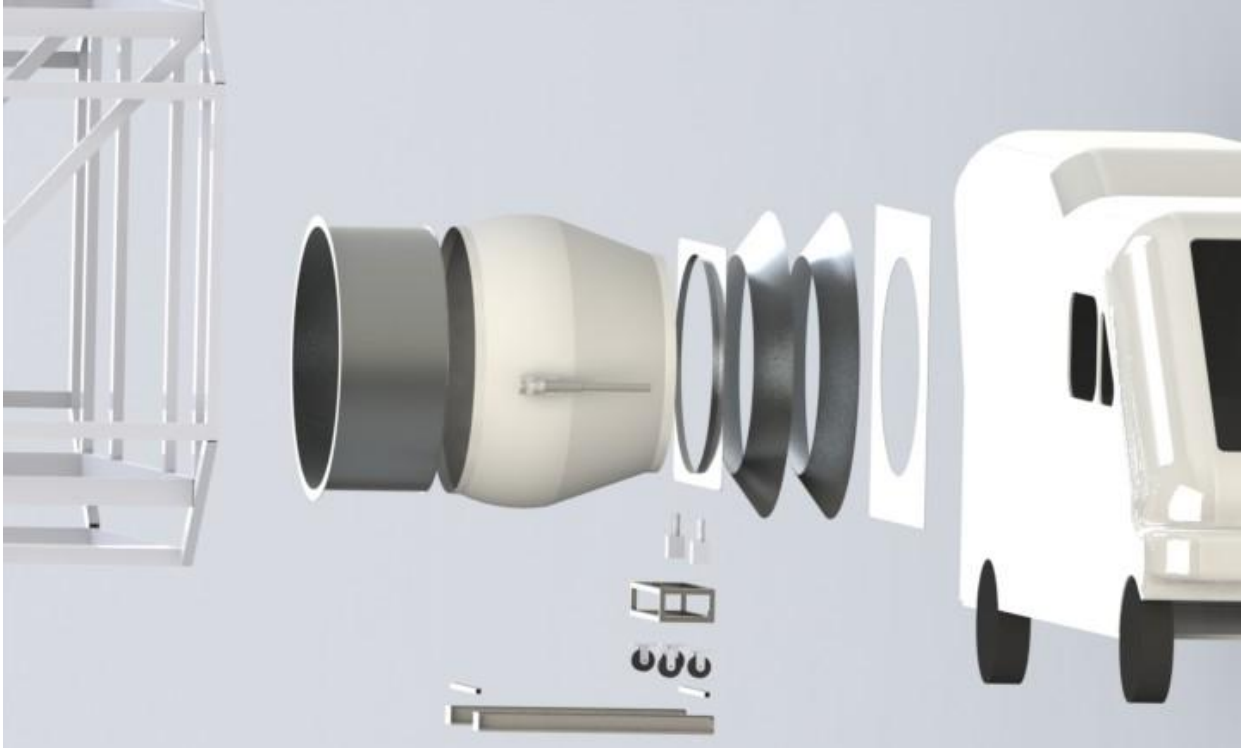
Fixed Section of Tunnel

The fixed section of the tunnel is .5 meter, 19.7 inches, long, with a diameter of 1.2 meters, 47.2 inches. On the side attached to the ILH there is a 6 cm, 2.4 inches, lip to allow attachment points. On the side toward the extendable section of the tunnel there is a 3 cm, 1.2 inches, lip to allow attachment points for the bladder.   This component was made of steel and built locality. This component is there to allow attachment points between the ILH and the expandable section of the tunnel and to supply structural strength to the overall structure.
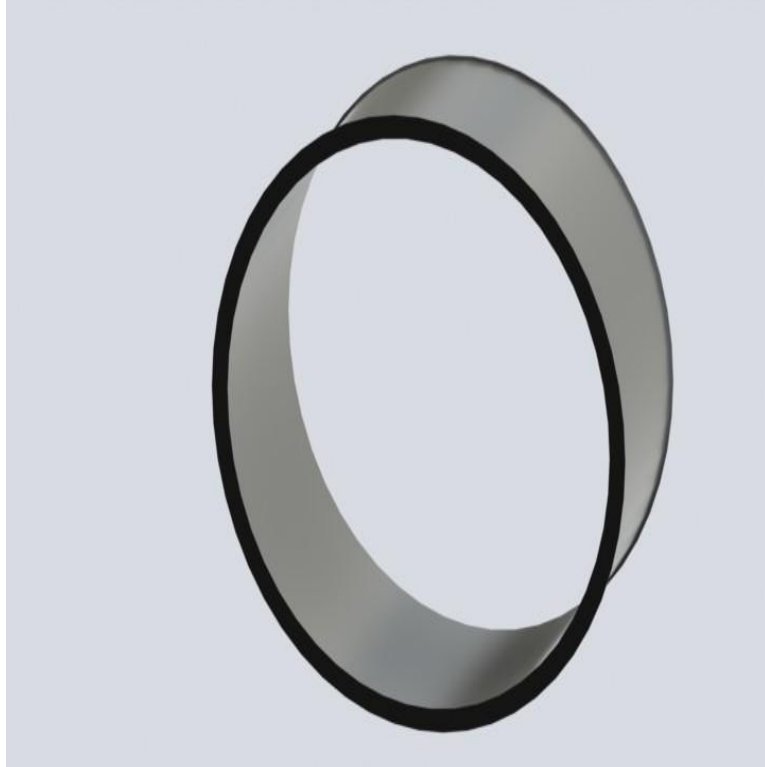
Figure 32: Fixed Section of the Tunnel

This covers half the distance of the tunnel.

Tunnel Side Female Mating Ring

The mating rings are very important parts of the tunnel system. The rings help with the adjustment between the tunnel and the rover. The mating rings help guide the openings to line up with one another. The ring that is at the end of the expendable section of the tunnel is the female side of the two mating rings. When it expands and mates with the other ring the tunnel side ring goes on the outside of the rover side mounting ring. The tunnel side ring also has attachment points for the latches that will provide the locking and structural support once the tunnel is docked. The dimensions are shown in Figure 33. The ring is made of aluminum and is mounted on a square

sheet of aluminum with a circle with a diameter of 1 meter, 39.4 inches, cut into it. At

each of the corners is an attachment point for the connection rods which is the male

end of the latch system. Around this cut is a 4 cm, 1.6 inches, lip that the bladder will

attach to. On the bottom of the square piece is a flat rectangle piece of aluminum to

allow attachment to the vertical linear actuators. There are no sharp edges on this part;

every corner is rounded so there is nothing that can damage the bladder by accident.

The mounting plate it is welded to is a square of .26 cm or .101 in of thick aluminum

with a height and width of 1.09 meters. This mounting plate has space for the four

mounting points for the connection rods of the latching system at each corner of the

mounting plate.
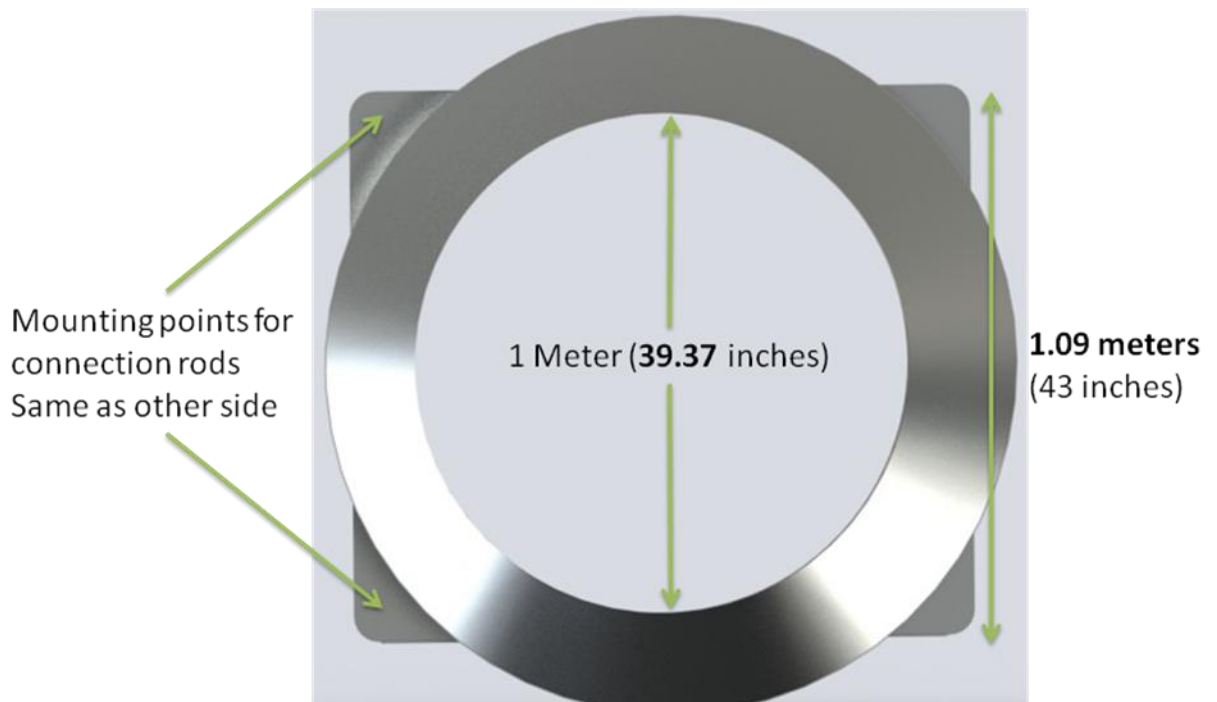
Figure 33: Tunnel Side Female Mating Ring

Cart and Rails

To allow the tunnel to move the .5 meters, 19.7 inches, 363 kg, that it is designed to and still have the ability to rise up and down a cart and rail system has been designed. Casters that can support up to 800 pounds, and have a v groove, have been used on a rail to move the cart back and forth.

Figure 34: Rigid Caster with v-groove from Granger Technical Specification

These casters are on a rail that is a solid .5 in diameter, 0.0127 meters, steel rod that is attached to a 1 x 2 inch, 2.5 x 5 cm, rectangle steel tube. The casters sit on the rod that is a cylinder so if there is any dust buildup it will slide off. Over time, maintenance will have to be done so dust cannot build up on the rectangle steel tubing that supplies the support to the rod.
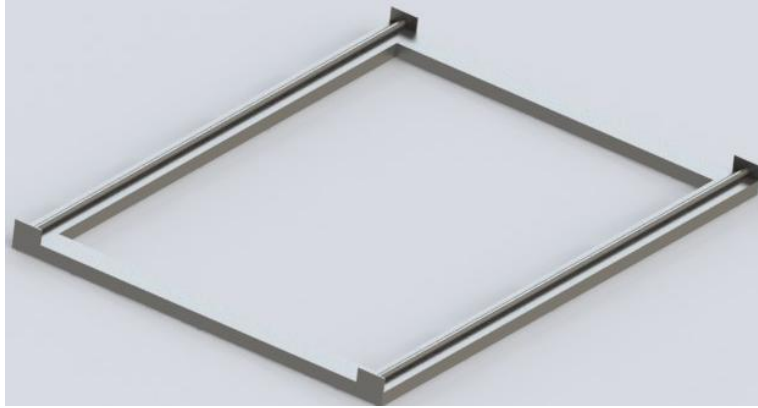
The cart is a simple box of square 1 inch, 2.5 cm, steel tubing. This cart will supply the mounting points for the vertical linear actuators and the casters to move back and forth on the rails.
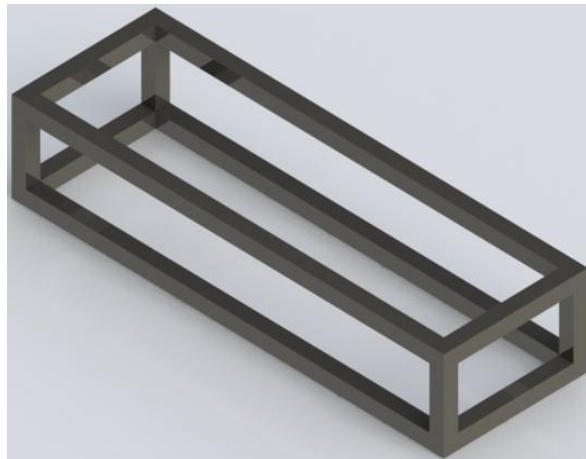
Figure 36: Cart Frame

The frame is 76 cm by 15 cm by 25 cm deep or 30 inches by 6 inches by 10 inches.

Figure 37: Cart on Rails

Rover Side Male Mating Ring

The rover side male mating ring is mounted on one side of the rover. It is fixed in its position and bolted to the metal structural of the rover. This ring is a twin to the ring used on the tunnel side. This is so both rings will fit into each other exactly. The diameter of the opening is 1 meter or about 39 inches. The height and the width is 1.42 meters or about 56 inches. The mounting plate that will allow this ring to be mounted on the rover is a square except for the left hand side top corner. This corner is cut to prevent the mounting plate from overlapping the driver side window of the rover.
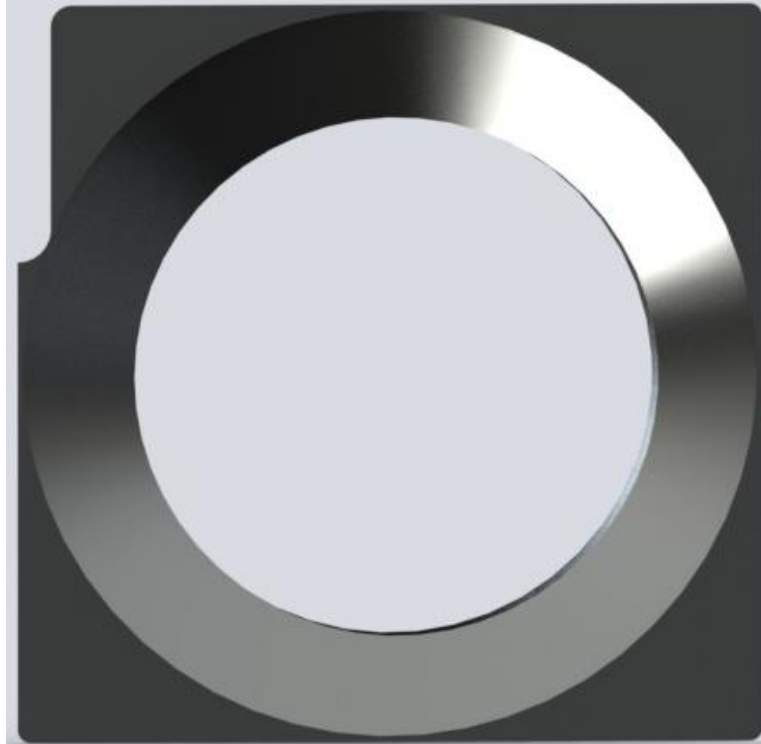
Figure 38: Rover Side Ring System

3 Doors

There are three different doors associated with this tunnel.   Two of the doors are very similar to each other: the door on the rover and the door on the inside of the tunnel. The door on the rover is 1 meter, 39.4 inches, in diameter, while the door on the inside of the tunnel, with the ILH is 1.2 meters, 47.2 inches, in diameter. Both are constructed about the same way, out of fiberglass, with a 15 cm, 5.9 inches, hole in the center to allow for a window. The third door is a zipper fabric door at the end on the tunnel. This door is to keep rain, snow, ice, and other weather out of the tunnel. Once the docking process is over, the crew inside the rover can open their door; unzip the fabric door then proceed into the tunnel to the ILH.

Bladder

The bladder is made of up three layers of fabric similar to that of a space suit or the fabric of the ILH. The three layers, starting with the inner most, are: the bladder, the restraint layer, and the thermal and dust protection layer.   The bladder is there to contain the atmosphere of the ILH. The restraint layer is there to keep the bladder in the shape needed to keep the tunnel functional.   The purpose of the thermal and dust protection layer is to insulate the tunnel and protect the bladder and restraint layer from corrosion from dust, weather, and wind. There is a gasket at both ends of the tunnel to seal the bladder to the metal elements of the structure of the tunnel.

Structural Analysis

To ensure that the tunnel will be able to support the weight of a human in a space suit, a generalized weight of 300 pounds (1334 newtons) for a human in a space suit will be used. The designing factor of this tunnel is to have a factor of safety of 3. Factor of Safety is Equation 44:

Equation 44

$$n = \frac{Allowable\ force}{Calcuated\ force}$$

The calculated stress will be 300 pounds (1334 newtons); the allowable stress will be three times the calculated stress of 900 pounds (4003 newtons) (Budynas, 1977).

Now during the design and the analysis of the design a force of 900 pounds (4003 newtons) is used to allow the load bearing components to have a factor of safety of 3. In this section a structural analysis of the components that will be put under stress by the force a human in a space suit crossing through the tunnel.

Hard Section of the Tunnel fixed to the ILH

The Hard Section of the Tunnel and the cart will be supporting the weight

Rails are fixed to the ground
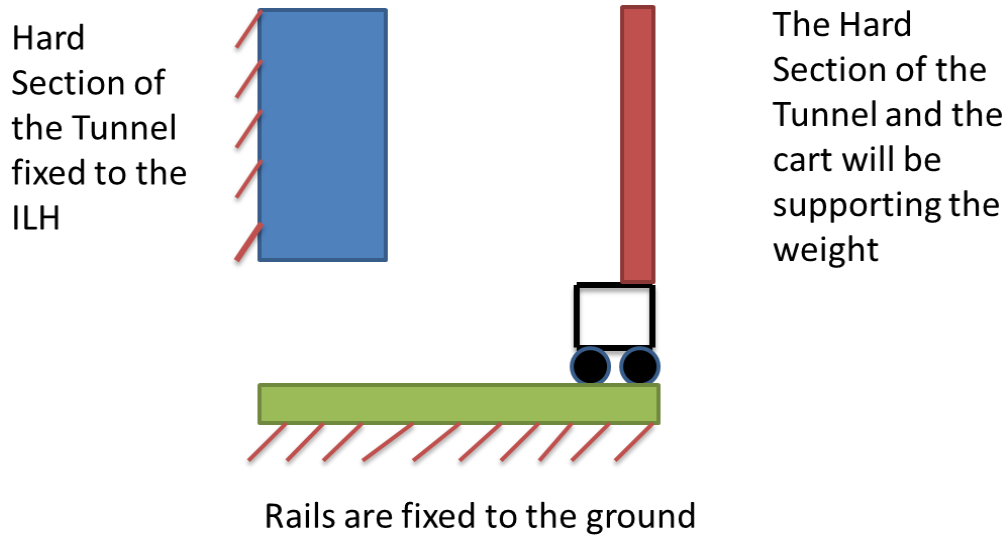
Figure 39: Simplified drawing of force supporting components

The first of the components that will have to be analyzed is the hard section of the tunnel. The following **Error! Reference source not found.** contains all the properties of the hard section of the tunnel.

Table 4: Properties of the Hard Fixed Tunnel Section

Item	Metric Units	English Units	
Diameter	1.2 meters	47.24 inches	2r
Thickness	. 256 cm	0.1011 inches	t
Length	.5 meters	19.69 inches	L
Structural Steel ASTM-A36			
Specific Weight	7861 kg/m^3	0.284 lb/in^3	
Weight	33.2 kg	73.27 lb	
Young's Modulus of Elasticity	200 GPa	29 X 10^ 6 psi	E
Moment of Inertia	0.0137 m^4	33,014 in^4	I

82

To solve this problem the equation for beam defection for beam theory equations must be applied.
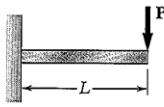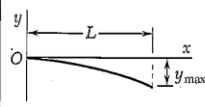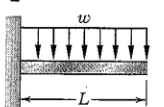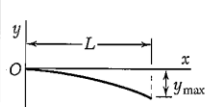
Beam and Loading	Elastic Curve	Maximum Deflection	Slope at End	Equation of Elastic Curve
1		$-\dfrac{PL^3}{3EI}$	$-\dfrac{PL^2}{2EI}$	$y = \dfrac{P}{6EI}(x^3 - 3Lx^2)$
2		$-\dfrac{wL^4}{8EI}$	$-\dfrac{wL^3}{6EI}$	$y = -\dfrac{w}{24EI}(x^4 - 4Lx^3 + 6L^2x^2)$

Figure 40: Beam Deflections and Slopes (Beer, Johnston, & DeWolf, 2003)

The second row down shows the force distributed over the length of the beam. The tunnel can be treated like this. The equation for the maximum deflection is Equation 45:

Equation 45

$$D_{max} = \frac{-wL^4}{8EI}$$

Moment of Inertia for the hard section of the tunnel can be found by Equation 46:

Equation 46

$$I = \frac{1}{4}\pi r_{out} - \frac{1}{4}\pi r_{in}$$

Using Equation 45 the maximum deflection at the end of the tunnel hard section that is not fixed to the ILH is 0.00000735 inches (1.8669 × 10^{-5} cm). This number is so small that for this thesis it is assumed that there is no deflection in the hard section of

83

the tunnel. A 300 lb (134 kg) person including his or her space suit has a factor of safety

of 3 when in the hard section of the tunnel.

The next component that requires a structural analysis is the cart. The cart is the

other load bearing structure of the tunnel.   Compressive forces are will be acting on the

cart and the design of the cart took this into consideration. A careful analysis of the cart

has to be undertaken to check for failure modes such as crippling, local buckling,

buckling and, fracture.

The first failure mode to check is to see if the stress caused by the compression

force is over the critical stress for the member. Axial stress in the cart can be found by

Equation 47:

Equation 47

$$\sigma_x = \frac{P}{A}$$

Using the steps set forth for allowable stress design in the Allowable Stress

Design Specifications of the American Institute of Steel Construction (AISC) (American

Institute of Steel Construction, 1989), it can be shown that the cart is not under any

threat of any failure mode from the applied force. A parabolic expression can be used

to predict σ_{all} (stress for the entire member) for all columns of short and intermediate

lengths, in this case it is for a short column (Beer, Johnston, & DeWolf, 2003). Figure 41

shows a curve that represents the variation of σ_{cr} (critical stress, where the member

starts to deform due to the applied load) with L/r, the length compared to the radius of

the member.
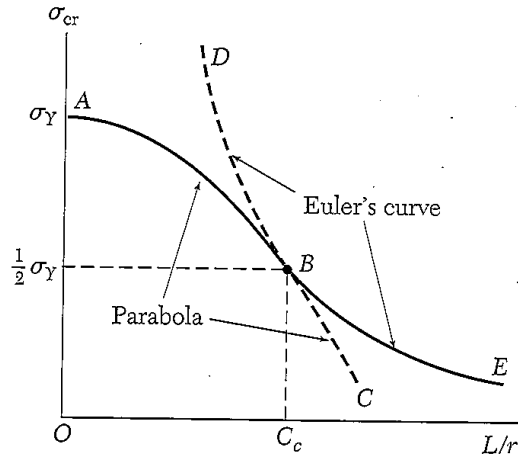
Figure 41: Allowable Stress Design (Beer, Johnston, & DeWolf, 2003)

The AB section of the curve is an arc of a parabola that is defined by Equation 48:

Equation 48

$$\sigma_{cr} = \sigma_0 - k\left(\frac{L}{r}\right)^2$$

Section BE is part of Euler's curve DBE that is defined by Equation 49:

Equation 49

$$\sigma_{cr} = \frac{\pi^2 E}{(L/r)^2}$$

It is assumed in the AISC document that at point B, where the parabola joins Euler's curve that the critical stress is equal to half of the yield stress and C_c is the L/r at that point (Beer, Johnston, & DeWolf, 2003). By using Equation 49 the critical stress is found to be 4,470,000 psi (30.8 GPa) and assuming C_c is L/r of the cart the yield stress is 8,940,000 psi (61.6 GPa). Using Equation 47, the stress of the applied load is 2,058 psi (14,200 KPa). This is significantly under the values of the critical stress and the yield stress. This means that there is not enough force applied to the cart to cause failure.

85

The factor of safety for this one component for failure due to fracture is over 4,000.

This is much beyond the design parameter of a safety factor of 3. This proves that the

applied design load will not cause failure in the cart.

Buckling

When a member is under a compression force, such as the vertical bars of the

cart in the relationship with the weight of the tunnel above it, there is the chance that

the member can bow out in the middle and cause the structure to deform. This is called

buckling (eFunda, Inc., 2012). Buckling leads up to a failure mode. It can be used to

predict when failure is close to occurring. To figure out what force is required for this to

happen to the cart, Equation 50 called the Euler's formula is used.

Equation 50

$$F_{cr} = \frac{EI\pi^2}{L^2}$$

The Moment of Inertia (I) can be found by using Equation 51:

Equation 51

$$I = I_{outer} - I_{inner} = \left[\frac{bh^3}{12}\right]_{outer} - \left[\frac{bh^3}{12}\right]_{inner}$$

The Moment of Inertia is found to be 0.057 in^4 (2.37 cm^4) . The length (L) of the

member is 4 inches; Young's Modulus of Elasticity (E) is 29 * 10^6 psi (200 GPa). The

critical force is then found to be 1,019,654 pounds of force (4535647 newtons). This is

much larger than the applied force of 900 pounds (4003 newtons). This number is so

large because buckling usually only affects long columns. The reason is that this

member is so short it will fracture before it is able to buckle.

Local Buckling

Local buckling is the same as normal buckling except it is localized to one area of the member, where buckling affects the entire column.

Where P is the force applied to the section of the structure and A is the area of the section of structure.

To figure out the critical stress where local buckling occurs there is a design chart and equation to aid with this problem, the graph is shown in the following Figure 42 (Bruhn , 1973):
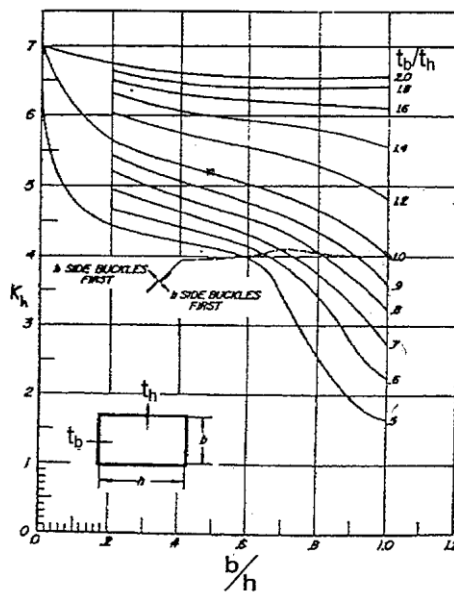
Figure 42: Rectangular-tube-section (Bruhn , 1973)

The equation that goes along with this as follows:

Equation 52

$$\sigma_{cr} = \left(\frac{k_h \pi^2 E}{12(1 - \nu_e{}^2)} \right) \left(\frac{t_h}{h} \right)^2$$

Table 5: Properties of Structural Steel, ASTM-36, used to create the cart frame

	Symbol	English Units	Metric Units
Buckling Constant	k_h	4	4
Poisson's Ratio	ν	0.29	0.29
Thickness of the top section	t_h	1/8 in	0.3175 cm
Height of the section	h	1 in	2.54 cm
Young's Modulus of Elasticity	E	29 x 10^6 psi	200 GPa

Poisson's Ratio:

Equation 53

$$\nu = -\frac{lateral\ strain}{axial\ strain}$$

The Poisson's ratio used in this computation is 0.29 (Sokolnikoff, 1983).

If the critical stress for local buckling is higher than the stress applied to the structure then there is no chance of local buckling in the member. After substituting all the values into Equation 52, the critical stress for local buckling is 1.625 x 10^6 psi (11.2 GPa). The axial stress is only 2058 psi (0.014 GPa). This means that local buckling will not occur under the applied design load.

Crippling

During design tests of short sections of a member it has been shown that after local buckling has occurred, the member can still carry a greater load before failure occurs. This means that local buckling and the failing stress or crippling are not the same. For cases when local buckling happens at lower stresses, the failing stress or crippling will be higher. But for cases when local buckling occurs at .7 to .8 of the compression yield stress it can be assumed that buckling and crippling are about the same (Bruhn , 1973). For ductile metals the compression strength is generally assumed to be equal to the tension strength (Beer, Johnston, & DeWolf, 2003).

Using the Gerard Method for crippling stress calculation, this was established after a comprehensive study of published theoretical and experimental results. This method presented a generalized method of determining crippling stresses (Bruhn , 1973).

The equation for sections with distorted unloaded edges such as angles, tubes, V groove plates, and mulit-corner equations used the following Equation 54:

Equation 54

$$\frac{F_{cs}}{F_{cy}} = 0.56 \left[\left(\frac{gt^2}{A} \right) \left(\frac{E}{F_{cy}} \right)^{1/2} \right]^{.85}$$

Using Equation 54 F_{cs}/F_{cy} can be found to be 7.97. To check that this is right a chart of the design curve for F_{cs}/F_{cy} vs. $\left(\frac{A}{gt^2} \right) \left(\frac{F_{cy}}{E} \right)^{.5}$ has been provided.
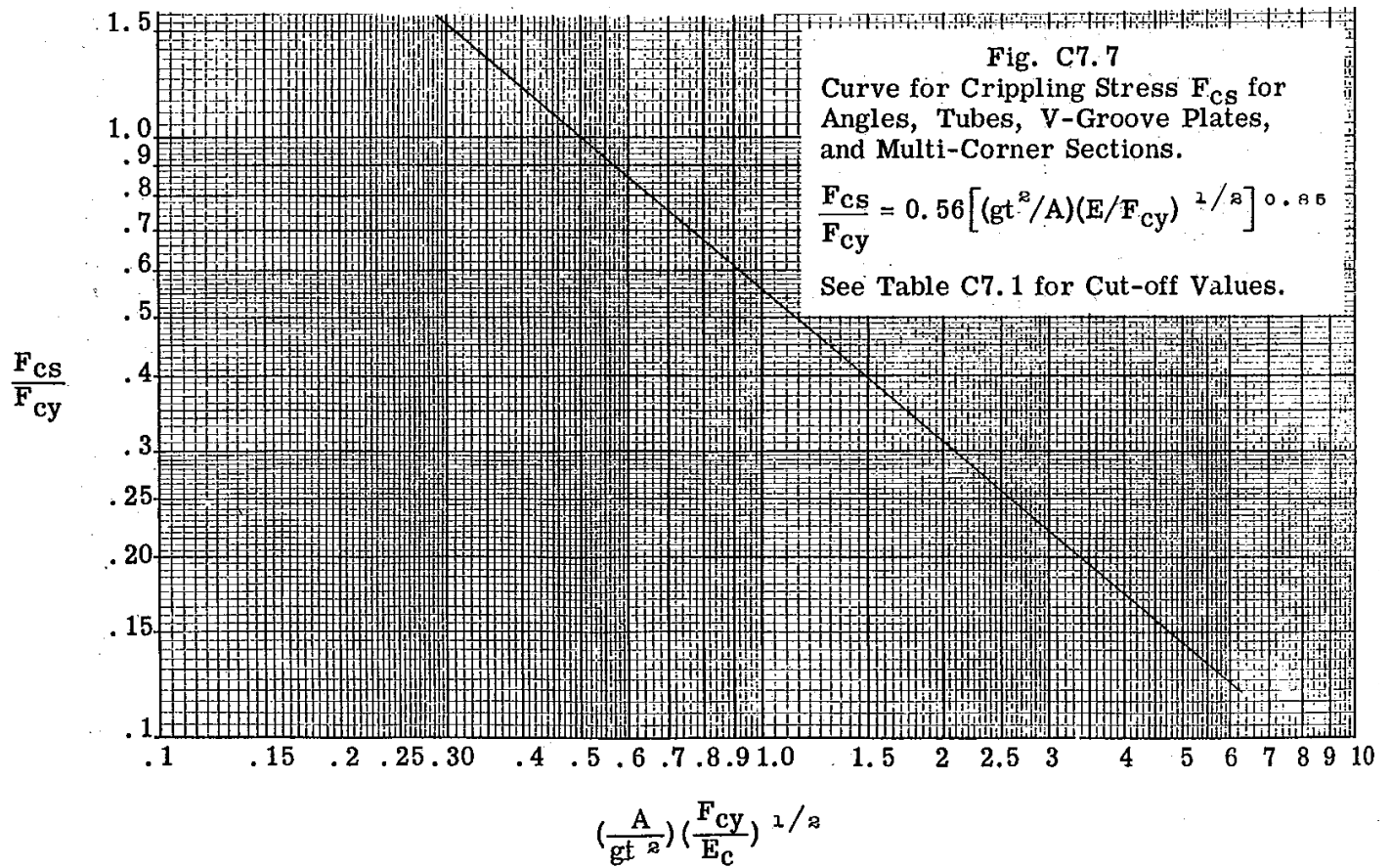
Figure 43 : Design Curve for Crippling of Tubes (Bruhn , 1973)

After looking at Figure 43 it can be seen that this value is not on the design

curve. There are cut-off values for the maximum crippling stress for the section. These

values can be seen in **Error! Reference source not found.**.

90

Table 6: Cut-off Values for Crippling (Bruhn , 1973)

Type of Section	Max. F_{cs}
Angles	$.7\ F_{cy}$
V Groove Plates	F_{cy}
Multi-Corner Sections, Including Tubes	$.8\ F_{cy}$
Stiffened Panels	F_{cy}
Tee, Cruciform and H Sections	$.8\ F_{cy}$
2 Corner Sections. Zee, J, Channels	$.9\ F_{cy}$

After looking at **Error! Reference source not found.** it can be seen that the cut-off

value is $.8F_{cy}$, looking at what was found from Equation 54 that $F_{cs} = 7.97F_{cy}$ way over the

cut-off value, so in this case the cut-off value is used instead.   The cut-off value is found

to be $.8F_{cy}$= 28,800 psi (.2 GPa). The cart is only designed for 900 lb$_f$ or 3846 psi of

stress. To find the factor of safety for just the crippling stress is 22.5. This is much over

the design goal of a crippling stress factor of safety of 3. This means that crippling will

not occur while the cart is under the applied design loads.

Control System

The PER will never park in the exact same spot when it returns to the ILH after a

mission. There needs to be a way to adjust the tunnel so it can dock with the PER no

matter what position it docks in. With more weight in the PER's suspension will sit

lower to the ground. Using parking chalks, like at airports, to help align the parking

position, a laser guidance system to align with the tunnel, a viewing system to watch the

docking process, and a system to control the adjustment of the tunnel is all part of a

system that works together to ensure that the PER can dock with the tunnel.

What is a Control System?

The simplest way to think about a control system is that there is a physical

quantity that must be controlled to ensure that it becomes the wanted value

(Mastascusa, 2002). There are four keys to understanding how a control system works:

what you want the system to do; what you tell the system to do, called the input; how

well the system is performing (the feedback); and how to react to how the system is

performing, called the output (Mastascusa, 2002).
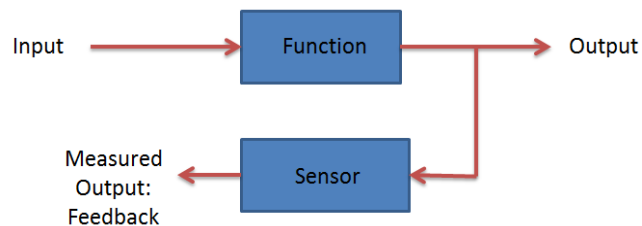
Figure 44: Control System Block Diagram by Timothy J. Holland

A control system is needed to control the movement of the tunnel in a safe

manner that will maintain its operational capability.   The manual command tells the

linear actuators what the operator wants them to do, then the viewing monitoring tells

the operator how the system is performing, and then the operator can readjust the

manual command to react of how the system is performing.

Due to the different weights that the PER will be transporting during its missions, the suspension of the rover will be at different height levels. To overcome this problem, the tunnel must be able to move up and down in the vertical direction.   Linear actuators have been chosen for this task. A linear actuator is an electro-mechanical machine device that creates motion in a straight line by converting rotary motion to linear motion by rotating the actuator's nut to move the screw shaft in a line (Gill). The movement of each linear actuator is controlled by a manual command in the control box.

The linear actuator that was chosen for this task is the Duff-Norton LT225-1-100. It is rated to a load of 225 lbs or 1000 newtons with a stroke length of 100mm or 3.9 inches. It has voltage of 12 VDC, current of 3.5 Amp Max, and a duty cycle of Max. 25%/2min/6min. This linear actuator has the ability to raise the tunnel ring up 100 mm or almost 4 inches to fine tune the alignment.   Two of these will work in tandem to rise and lower the tunnel ring.

Horizontal Control

Horizontal movement is controlled in a manner similar to that of the vertical control method. Both use linear actuators and are controlled by a manual command at the control box. But the horizontal movement required is farther and thus requires a longer linear actuator. The linear actuator that has been chosen for this task is a Duff-

Norton LS35-3B4TN-24 that has 12 VDC, a force of 675 lbs or 3003 newtons, and a

stroke length of 24 inches or 61 cm.

Viewing system

The viewing system will be an off-the-shelf video camera and monitor with IR

capability. Infrared technology is necessary because the camera has to work in any light

condition, including total darkness. A full explanation of infrared technology and the

capability of the camera follows.

Infrared light is classified as non-visible light on the light spectrum. There are

three different categories of infrared light: near-infrared (near-IR), mid-infrared (mid-

IR), and thermal-infrared (thermal-IR). Near-IR and mid-IR are used by many different

electronic devices such as remote controls. Thermal-IR occupies the largest part of the

infrared spectrum with its wavelengths from 3 microns to over 30 microns (Morovision

Night Vision, Inc.).

The infrared cameras have detector and lens combinations that give a visual

representation of infrared energy that is emitted by objects in its viewing area. Thermal

infrared images allow heat to be viewed and see how it is distributed. The IR camera

detects infrared energy and converts it into an electronic signal that is processed to

create a thermal image (Thaller). The lens of an IR is similar to that of a visible light

camera, but the lens focuses waves from infrared energy onto an infrared sensor array

(Thaller). Thousands of sensors on the array convert the infrared energy into electrical

signals that are then converted into an image that can be viewed the same as an image from a visible camera (Thaller).

There are two types of thermal-imaging devices: un-cooled and cryogenically cooled. Un-cooled are the more common type of thermal-imaging cameras. It operates at room temperature (Morovision Night Vision, Inc.). The other type is cryogenically cooled. In this project, the camera used is un-cooled.

This type of night vision is better than traditional night-vision equipment that uses image-enhancement technology because it works well in near-absolute darkness with little or no ambient light (Morovision Night Vision, Inc.).

The camera will be mounted on the outside of the tunnel to view the docking process. The camera will send its feed inside the ILH to the control box where a monitor will be located. On the monitor, a grid will be utilized to help with the alignment of the tunnel ring with the PER ring.

Laser Guidance System

The laser guidance system is comprised of two different lasers. The first laser is the laser rangefinder. This is described in the sensors section. The other laser is a high powered laser pointer. The laser pointer is mounted in the rover on the driver side, the same side that the tunnel will dock with. The laser will shine on a grid that is attached to the fixed section of the tunnel, so the driver of the PER can adjust it to ensure the correct parking spot for capture of the PER by the tunnel.

Parking chalks/areas

To assist with parking the PER in position to dock with the ILH, a set of parking chalks are utilized. These parking chalks are set up so that when the PER comes to position itself to dock with the ILH it will be easier to line up. The most common form of parking chalks are the kind seen in parking lots as in Figure 45:
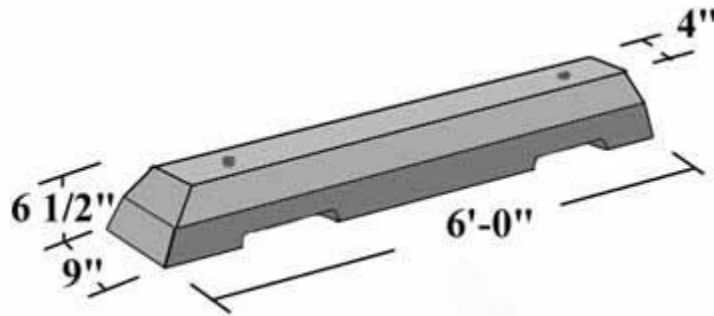
Figure 45: Parking Chalk from http://www.steps-plus.com/parking.htm

Another common use for parking chalks is at airports to stop the planes from going into terminal, align better with the jet-bridge. In this case the parking chalk will help align the PER with the tunnel. Shown in the following Figure 46 the layout of the parking chalks in relation with the IHR.
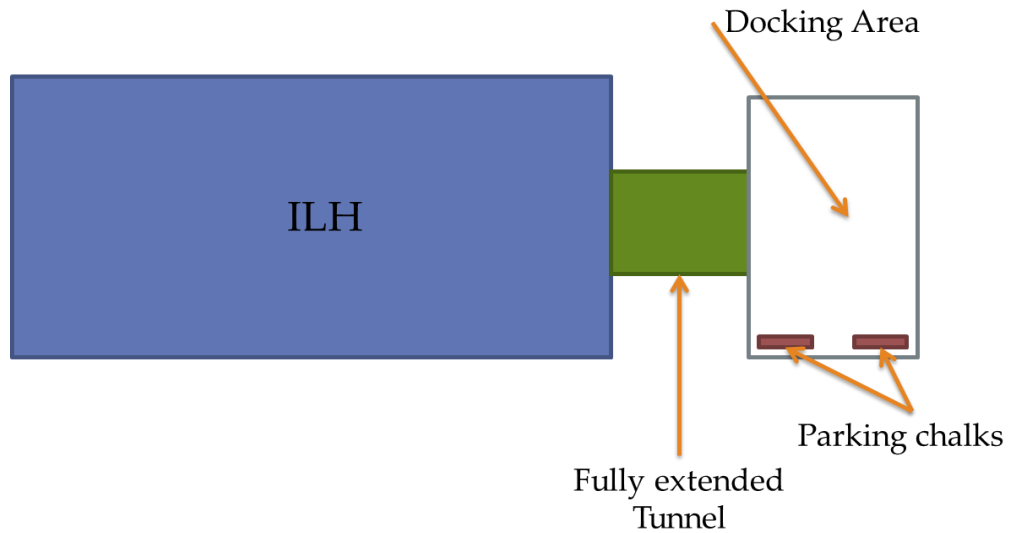
Figure 46: Diagram of docking area

Contact Sensors

Contact sensors are important in the docking process. To know when capture is completed, contact sensors in the latch system signal when this happens. These small switches close a circuit when they are pressed to a certain degree; this allows it to know when contact is made. Once the sensor reads that contact is made, a signal is sent to the control box which turns on a small indicator to inform the controller that there has been capture of the PER.

Control Box

The control box is the operational center of the control system. The control system controls the movement of both sets of linear actuators. From the control box the operator uses four manual actuators to maneuver the tunnel to line up with the

rover. Each individual manual actuator controls the movement of one of the linear actuators. The control of the manual actuator by the operator is the input. The sensors, providing feedback, are the laser range finder, the camera and the contact sensors.

The control box used is the Bud Industries Inc. Plasticase Style F PC-11495. It is an enclosure with plastic on the bottom and sides with aluminum to make up the front of the enclosure. It has a horizontal and vertical display area and a cable access panel in the rear. It came complete with all assembly hardware, including four rubber feet. It is made of durable UL94-HB rate ABS material and it is easy to modify with the tools that are in the Human Spaceflight Lab. More details can be seen in the appendix of this thesis about the control box.
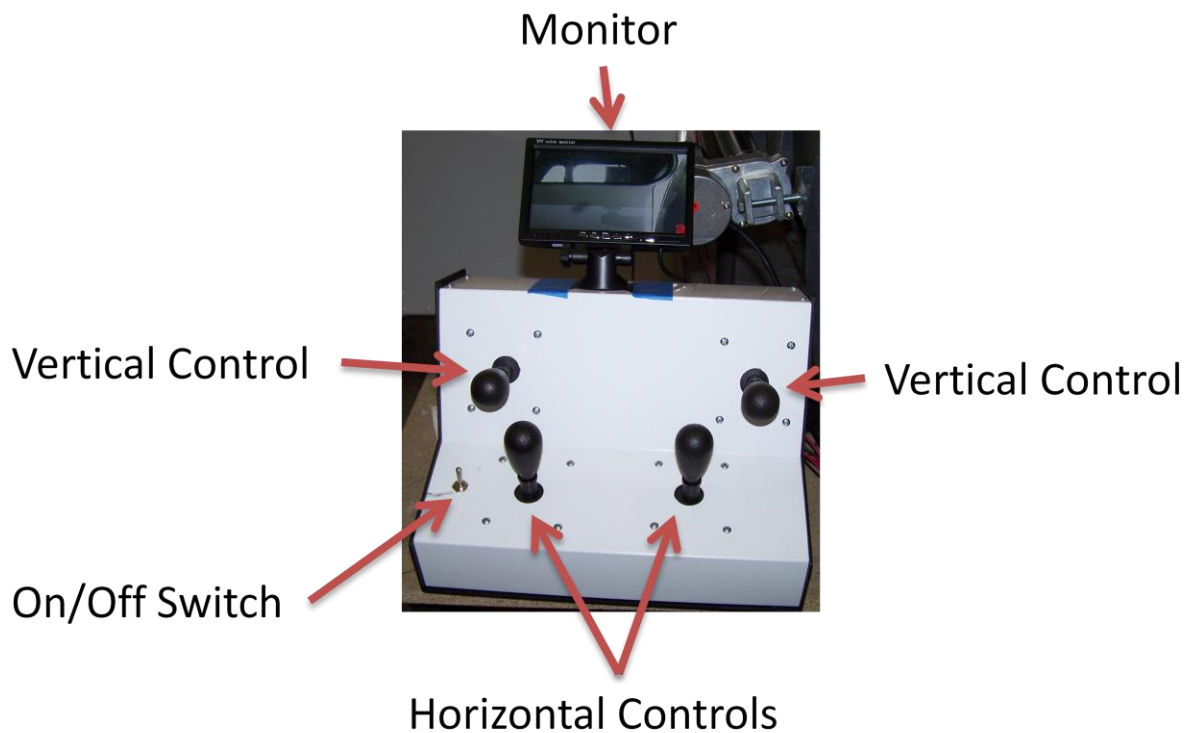
Figure 47: Control Box

To control the four linear actuators, there are four manual controls mounted in the control box. Each control stick is linked to one of the linear actuators. There are two different levels of the control box; horizontal position and vertical position. The manual controls on the horizontal control the horizontal linear actuators and the manual control on the vertical control the vertical linear actuators.

This control box will also house the indictors that will light up when contact is made during the docking process and when there is capture with the latch system. A monitor will be mounted nearby that will show the video feed from the camera. A communication system will also be set up close by so the operator can communicate with the crew inside the rover. The control box will be in the ILH.

Latch System

The latch system for the docking and securing mechanism on the tunnel is designed to be a simple system. It will be manufactured with cooperation from the Flight Robotics Lab at the National Aeronautics and Space Administration's Marshall Space Flight Center in Huntsville, AL. Instead of using a peripheral docking system that is complex, the latch system uses a modified four point latch system. The securing mechanism is mounted on the tunnel while the receiving mechanism is on the rover. This set up is similar to a central docking system, but there will be four of them around the tunnel entrance. This allows the utilization of a more simple central docking system and the ease of transport that peripheral docking system provides. This type of system is not used in space because of the weight, but on Earth, in analog missions, weight is

not necessarily a driving design factor. Figure 48 shows the latch system with the rod

captured.
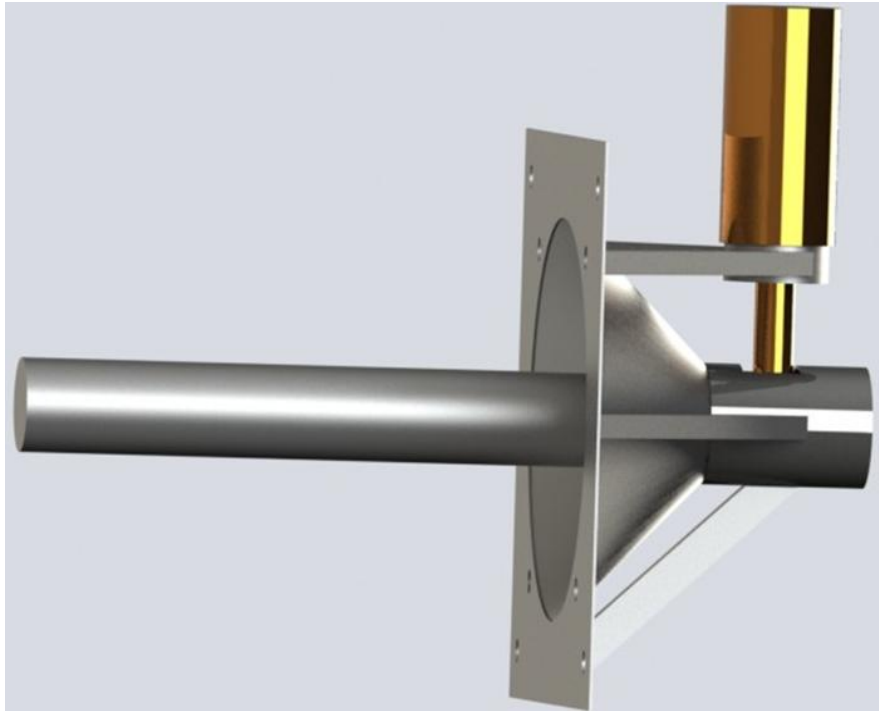
Figure 48: Latch System with rod captured

There are three main components of this latch system, the attachment rod, the

receiving cone, and the electromechanical solenoid. The attachment rod is mounted on

the tunnel on the edges of the female tunnel side ring mount, at each corner. The job of

the rod is to be the anchor point of the connection between the tunnel and the PER.

The receiving cone is built into the PER. There are four of them each corresponding to

an attachment rod.   The purpose of the receiving cone is to guide the rod into a

position where it can be secured.   The part that does the securing is the

electromechanical solenoid. An electromechanical solenoid is a coil of wire wound into

a tight helix. When electric is applied to the solenoid it creates a magnetic field. This

magnetic field affects the plunger or slug, the inner shaft of the solenoid that is made

out of iron or steel (Palmisano, ACTUATORS - SOLENOIDS, 2005). Depending on the

direction of the magnetic field the slug can either be attracted or repelled.
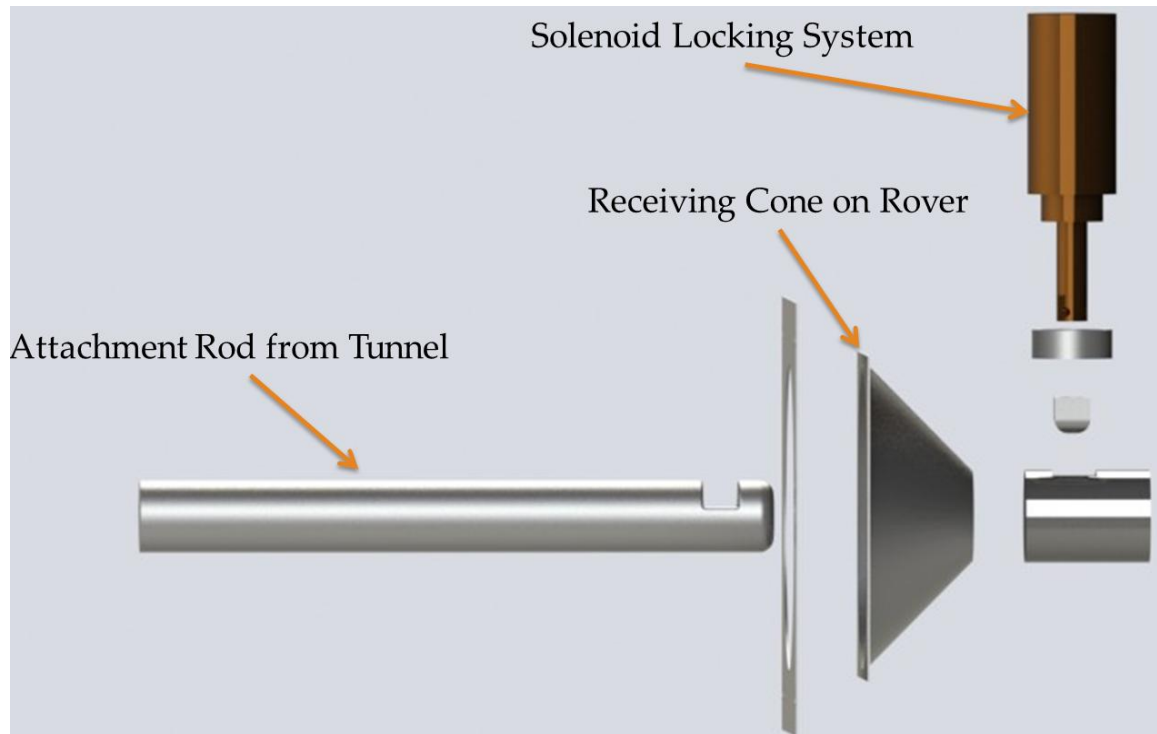
Figure 49: Components of Latch System

The rod is guided by the receiving cone into the capture area where the rod

compresses the end of the solenoid then moves deeper into the capture area. There is

a notch in the rod that will catch the end of the solenoid and thus lock the rod in

position.   For the rod to be released the solenoid is energized and the slug of the

solenoid is pulled up, unlocking the rod. This allows the rod to be pulled out from the

latch system.

Testing

Testing the prototype requires a number of steps. The first step is to set up a

test bed. The next step is to develop different testing scenarios based on realistic

problems that the system will face. All testing must be video recorded for future study

for integration into the ILH.

The first step is to develop a test bed. This test bed will be the tunnel hardware

as a standalone structure on the cinderblocks to get it to the actual height that it will be

when it is attached to the ILH. This will allow the testing of the tunnel without it being

attached to the ILH which is under construction. This will not slow the construction of

the ILH.

There are many different testing scenarios that can be considered for study. This

comes down to time allowed for testing. Some scenarios will just take too long for the

scope of this thesis. The weight of the payload is a major difference in scenarios

because the suspension changes with the weight inside the rover, this will happen every

time the rover is moved and thus it must be tested before the tunnel can be integrated

into the ILH. Weather conditions in analog mission can prove to be a challenge. On the

Moon there is no weather because there is almost no atmosphere, but on Earth where

the mission is taking place weather has to be considered. What weather conditions the

hardware needs to be tested in depends on when the analog mission is going to take

place. If it is in the winter, snow and ice have to be taken into account, while in the

summer, extreme heat and dust storms needs to be considered. Testing in North

Dakota's Badlands during eight months of the year snow and cold weather is a

possibility. Time of day will also be another important scenario because if the PER is

unable to dock at night that will be important information for the crew to know before

the mission starts. Different operators will have to be tested to see how much training is required for the docking process. Mechanical failure modes also will have to be tested, to know how these affect the overall mission.

Testing is extremely important, and testing of all scenarios will need to be done, but this is not in the scope of this thesis. This paper will only cover proof of concept testing. The tunnel will be tested to see if it can adjust enough to dock with the rover. In this phase of development only preliminary testing can be done, but more testing is required in the future to prove that the tunnel is ready to be integrated into the ILH. This will be done at a later time

Expected Results

While the expected outcome of the thesis is a proof of concept for a operational transfer system which will dock the PER with the ILH to allow easy passage of passengers from one to the other without need for spacesuits, there are a number of potential problems that could occur that will effect this expected outcome.   There are a number of anticipative problems for this process.

The anticipated problems could occur during the initial constriction and testing of the tunnel include: unavailability of needed components, mechanical failures, problems with interfaces of electrical systems, and control system failures.

Components are coming from a variety of sources. For example, the Marshal Space Flight Center is supplying the latch system and there has been limited contact

with them. For the level of testing in this thesis the latch is not required, because of the structural stability of the mating rings when they are mated.

There can be mechanical failure of various parts at any time during the build or testing phases. This is a fact of life and must be dealt with at the time, but it could add cost and time to an already tight schedule.

Assistance will be needed to ensure that the electrical systems are interfaced and working properly. A similar issue could be experienced with the control system. A mistake here could derail the entire project. Docking is not an easy procedure and work on both the rover and tunnel side is required for a successful conclusion.

Troubleshooting of any of the above problems is expected, but the critical issue is at what cost? The issues of money and design are real, but the most critical issue is time.

The expected result is that the tunnel will work as planned. Once the test bed is up and running and the proof of concept is successfully achieved, future research directions can be developed. Some ideas include: testing of the tunnel under more extreme conditions; integration of the tunnel with the ILH once that is built; testing of the tunnel in analog missions.

Chapter III
RESULTS

There have been a number of preliminary tests completed on the docking

system between the ILH and PER. The results have been positive, showing that this

prototype can perform its designed function.   In this section the results of the design,

analysis and testing will be discussed.

Design Changes

Since this thesis was originally planned there have been a number of design

changes. These have been put into place because the analysis of the original design

showed flaws in some areas. The two major design changes have to do with the

installation of guide rails for the tunnel side mounting ring on the cart.

Support Guide Rails

To keep the tunnel side mounting ring normal to the cart, it was discovered that

the original mounting system proposed was inadequate to support the tunnel side

mating ring. To overcome this problem, a set of guide rails was designed to offer more

support to the tunnel side mounting ring. These guide rails are mounted on an

extended section of the cart, about 11 inches or 28 cm from the end of the cart. These

guide rails are two pieces of angle iron that have a gap about double the thickness of

the tunnel side mounting plate. This allows movement up and down, and limits dust

build up that could affect the motion.

Figure 50: Cart drawing by Timothy J. Holland

The guide rails offer more controlled stability and movement of the tunnel side

mounting ring.

Figure 51: Photo of Cart with Guide rails

Mounting of the Vertical Linear Actuators

In the original design the vertical linear actuators were going to be mounted to

the cart, and provide support to keep the tunnel side mounting ring normal to the cart.

With the need for the guide rails, a new position to mount the vertical linear actuators

was discovered. Instead of having the vertical linear actuator push the tunnel side

mounting ring up from the bottom, the vertical linear actuators have been mounted on

the top of the guide rails. This is a much simpler set-up than the original design. Instead

of building an entire mounting system for the vertical linear actuators, only two bolts

were needed. One bolt to mount the vertical linear actuator to the side of the guide

rail, and the other bolt to attach it to the tunnel side mounting plate. This was

developed after contacting engineering support at Duff-Norton, the manufacturer of the

vertical linear actuators, to find out whether the linear actuators were better at pulling

or pushing. The engineers at Duff-Norton said that they were designed to do either at the same level.
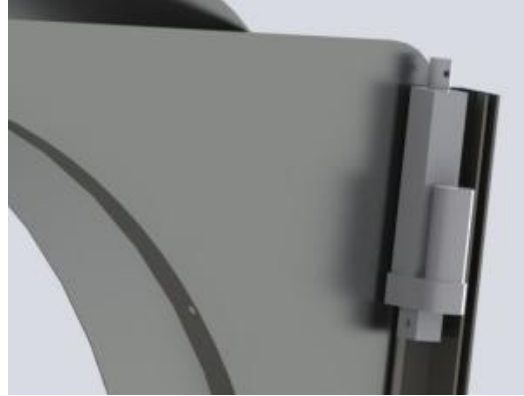
Figure 52: Drawing of Vertical Linear Actuator Mounting by Timothy J. Holland

Figure 53: Vertical Linear Actuator Attached to the Guide Rails and Tunnel Side Mounting Plate

This new mounting set-up for the vertical linear actuators is less complex, and able to be implemented by attaching directly to the guide rails.

Cart Stabilizer

The guide rails added more mass to the front of the cart. This moved the center of gravity of the cart very close to the front. The cart was only designed to support the mass of the vertical linear actuators and the mating ring set up.   This was expected, and a design change was set in place to counteract this immediately as the guide rails were designed.   The cart could not be lengthen to spread the casters apart more, because then it would interfere with the supports of the fixed section of the tunnel. Instead a screw was welded to the back of the cart to. At this point a 50 pound (23 kg) metal weight is placed there. This moves the center of gravity back to the center of the cart and increase stability.

Figure 54: Cart Stabilizer drawing by Timothy J. Holland

Testing

To validate the design, a series of tests had to be performed.   The tests evolve from a simple fit test, to testing the linear actuators, then testing the integrated tunnel system.

Fit Test

The fit test was the first test in the test process. To do this test the rover side ring was mounted to the rover. The tunnel side ring was also installed on the cart. The cart is then set up to have the center of each of the ring at the same point.   The cart is then moved forward and pressed against the ring on the rover. Once the two rings are mated it can be inspected of how well the fit is between the two rings.

The fit between the two rings is not perfect, due to the fact that the rover side ring has a slight bend in it. This slight bend will be straightened out by the installation of a metal bar in the rover and the mounting plate bolted to it. Other than that, the test was successful.

Figure 55: Photo of Fit Testing

Vertical Linear Actuators

There are two stages to testing the vertical linear actuators. The first stage is to hook up the vertical linear actuator to a power supply and test each one to see if they work to the intended specifications. This is done when they are not attached to the tunnel system. This test is to see if the actuators work on the specified length.

The second stage of testing is to attach the vertical linear actuators to the cart and test them to determine if they are able to move the tunnel side mating ring up and down. This was accomplished.

This test proves that the vertical linear actuators are going to perform to expectations.

Horizontal Linear Actuators

The testing for the horizontal linear actuators is similar to the vertical linear actuators. The first test was to see if the horizontal linear actuators perform as expected. This is where some issues came up. One of the linear actuators only extended half of its stroke length. The linear actuator would only extend 12 inches or 30.5 cm. This is not the expected stroke length of 24 inches or 61 cm. This limits the distance that the entire tunnel can extend. To continue testing, the distance that the tunnel will extend will have to be reduced to the maximum tested distance of the malfunctioning linear actuator, or only 12 inches.

This problem limits the movement of the tunnel, but it does not affect the testing validation that this tunnel design will work as a transfer system from the ILH to the PER. Due to time constraints, a replacement part could not be ordered in time, so the testing went forward with a limited capability of horizontal movement. It will operate as designed but only extend half the desired distance.

The second stage of testing, with the horizontal linear actuators attached to the cart and the fixed section of the tunnel, was successful even with the full extension limited to half of the proposed distance.

Combined testing

The next testing scenario is with both sets of linear actuators mounted in their final position. With both linear actuator sets integrated into the system, it was tested so that both sets operate at the same time. This scenario also calls for the tunnel to mate with the rover when it is in a fixed position.

This combined test showed that both actuator systems are able to function when integrated into the tunnel system and that the tunnel is able to mate with the rover in a fixed position.

Figure 56: Combined Tunnel Testing

Combined Testing with Bladder Mock-Up

One of the most repeated comments during the thesis proposal was that people had trouble visualizing how the bladder would work with the tunnel's mechanical system. The actual bladder was not ready for testing since it is currently being designed and manufactured with the help of ILC Dover.   To give the audience a sense of how the tunnel is going to look with the bladder installed, a substitute had to be found.   A 6 by 8 foot (1.8 by 2.4 meters) industrial vinyl tarp was cut in half into two 3 by 8 foot sections and taped from the tunnel side mounting plate to the fixed section of the tunnel. This gives the impression of a bladder installed on the tunnel. While unpressurized this will make it easier for the audience to visualize what the final tunnel configuration will look like.

A few tests were done to see if the bladder mock-up would stay on the tunnel as it moved: forward, backwards, up, and down. After some slight adjustments of the vinyl fabric, performed as expected.

Figure 57: Testing with Mock-Up Bladder
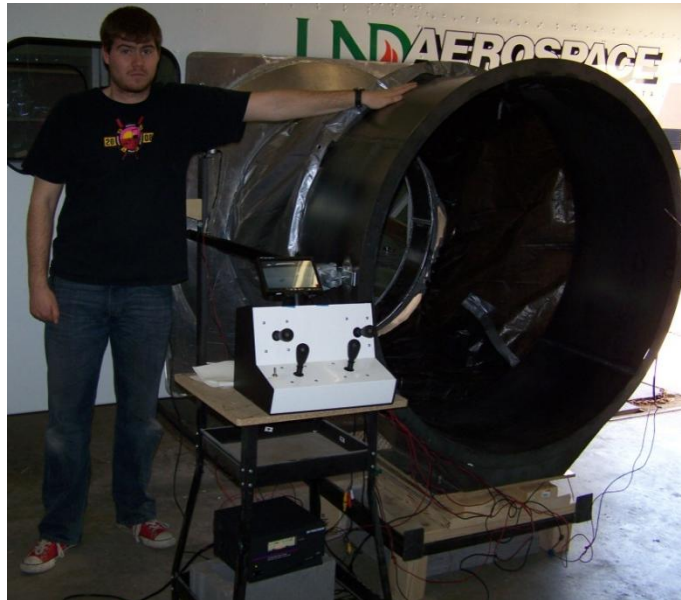
Figure 58: Tunnel with Mock-Up Bladder with Tim Holland for Scale

Figure 59: Tunnel with Mock-Up Bladder Docked with the PER

Combined Testing with Bladder Mock-Up and Video Sensor

Now, with the mock-up bladder installed, some of the sensor testing could be performed. Using the camera discussed in the Methodology section, some testing of the sensor has been completed.

A camera mount was built to secure the camera to the side of the moving platform. For testing purposes a provisional wood mount was built.

The camera is mounted about an inch (2.54 cm) from the end of the mount, which gives the camera a field of view with little of it being blocked by the tunnel side mating ring.

Figure 60: Pictures of Video Camera on Mounting Arm attached to Guide Rails on the Cart

This camera is linked to a video monitor that is mounted to the top of the control

box, to allow the operator a clear view of the tunnel operating.

Figure 61: Control Box with Video Monitor on Top

On the PER there is a target to allow the operator to have a reference to align the tunnel with the PER. Using this target with a grid on the monitor should allow the operator to align the tunnel with the PER.

This system performed as expected. Using a single operator to view the camera fed on the monitor, the operator was able to adjust the tunnel side mating ring from its highest vertical position to a position that allowed the two rings to mate when moved forward. It did take a few practice runs to get used seeing the target on the camera.

Problems

This design thesis has not gone without issues. There have been a number in this project. The first one discussed in this thesis was the malfunctioning horizontal linear actuators. There are a number of others as well.

Restructure of Testing Plan

The plan laid out during the proposal for this thesis was very ambitious. From the start of tunnel integration and final component fabrication in the Winter/Spring of 2012, it was already behind schedule. This proved that the proposed testing schedule was unrealistic, and a new testing plan to prove that the tunnel was operational was developed. This new testing program was set up to prove the mission operational of the tunnel system. By eliminating unnecessary testing that was designed more for show then to prove feasibility, the author changed the testing so it can be completed in a shorter amount of time without limiting results. By limiting testing to just operational testing and cutting out different scenarios, this thesis accomplishes everything set forward in the abstract.

Unfinished Control Box

The control box was the last component fabricated for this thesis. For the testing completed to date, the control box preforms as expected. However, the control box still requires additional parts that need to be added. What it is missing include the indicators to tell the operator that there has been contact between mating rings. Since the contact sensors have not been installed yet; neither have the indictors for them. Linear actuators move backwards if the current to them is reversed. There is a switch to reverse polarity, but it has not been installed in the control box. In order to have the linear actuators move backwards, the wires to the power supply have to be switched. These issues are small, and do not affect the overall performance of the tunnel, but once they are installed, will increase the ease of usability.

Limited Sensor Systems

In the design of the rover there are 4 sensor systems. For the level of testing that has been completed under the scope of this thesis only one sensor system has been operational. Testing here has only been with a fixed PER.   In the overly optimistic thesis proposal, it called for a number of tests involving the movement of the PER. As described earlier in this thesis, the testing completed for this thesis proves that the tunnel functional, therefore the extended testing of different scenarios is not need to prove the validation of the tunnel. Since the PER is in a fixed position, the laser guidance system is not needed nor is the laser range finder. The contact sensors are to be placed in the latch system. Due to unforeseen circumstances, the fabrication of the latch system with the help of MSFC has taken longer than expected. Without the latch system there are no contact sensors. In the next section, it is explained why the lack of a latch system does not halt all testing.

For the testing being performed for this thesis, only the video sensor is needed to perform the tests that have been described in the testing section.

Lack of Latch System

A complete working latch system has not yet been delivered. Fabrication is taking longer than expected, and the system would not be ready in time for the testing proposed. At first this seemed to be a major setback to the testing of the tunnel. As testing commenced, it could be seen that the mating of the rings along with the horizontal linear actuators created a stable structural support. The horizontal linear

actuators become rigid beams when they are turned de-energized, which secures the cart in its fixed position.   The same goes for the vertical linear actuators.   The rover side ring is fixed to the rover; the tunnel side has the horizontal linear actuators that are rigid connected to the fixed section of the tunnel. This keeps the cart in a stable position and, as seen in the structural analysis section of this thesis, the cart is structural sound under the applied design loads. With the rings mated, and the power turned off to the linear actuators, it becomes a rigid structure.

While this is may not be ideal for full analog operations, but for this level of testing it is adequate. It proves that the design and fabrication of the tunnel is operational. A latch system will improve the structural connection of the tunnel, but the tunnel's structural connection does not depend on the latch system. The initial testing without the latch system proves this.

Conclusion

This thesis covers the design and testing of an extendable tunnel between the ILH and PER. The design of a transfer system for analog planetary missions is something that has not been implemented before. This is an original approach to solving the transfer problem between the ILH and PER and will allow crew members to move between the ILH and PER without the need for pressurized suits. This approach eliminates a number of potential problems with future planetary exploration, such as loss of atmosphere during transfer and planetary dust, which have been discussed earlier in this thesis.

The work taken to prove this thesis included: research, analysis, and preliminary field/lab testing.

The start of the project required considerable research on the various docking configurations and mechanisms. A literary review was conducted to gather information about prior work in the field. This was covered in the introduction chapter of this thesis, and can be seen in the bibliography at the end of this thesis.

During the design process the author performed ongoing analysis of each component and configuration to be used in the tunnel. This was used to prove in the design stage that the tunnel components would be able to withstand the applied forces. In the Methodology chapter there is a section called structural analysis which goes into detail on the analysis of the tunnel components.

Preliminary lab/field tests confirmed the validity of the conceptual approach for the tunnel design. A step by step testing method was used. First a fit test was performed to see if the mating rings that were designed to fit together would in fact do so. This test was successful. Next, both sets of the linear actuators were tested to see if they could perform their required functions. Both sets were able to perform their duties. This was followed by combined systems tests where both linear actuator sets were tested after installation into the tunnel and controlled through the control system. The tunnel performed as expected and docking was successful. Next, using a tarp as a stand-in for the bladder, the tunnel once again docked with the rover. This test was also very successful. It gave insight on how the tunnel will behave with a fabric bladder attached to it. The final stage of testing was using a camera mounted on the tunnel to assist the operator dock the tunnel to the fixed rover using only what the operator

saw on the monitor. This also was successful. A detailed description of the testing and results is

contained in the Results section of this thesis.

There are a number of further changes and tests to be conducted on this tunnel. Future

work on the tunnel should include the installation of the bladder, upgrade of the cart, installing

a floor in the transfer tunnel, automatic docking capability, and weather proofing. Details of

these are in the future steps section in the Results chapter.

This thesis achieved its goals. The thesis proposal called for a more ambitious testing program

that this thesis did not get to for reasons covered in this thesis. The overall goal was to develop

an operational prototype for use with the analog system being developed in the UND Human

Spaceflight Lab. The preliminary testing covered by this thesis is more than enough to prove

that the transfer system that was designed and tested is a viable operational prototype for this

analog system.

Lessons Learned

This thesis is a learning process. There have been a number of things that, with

hindsight, could have improved.

Set Realistic Goals

The proposal of this thesis called for a very ambitious building and testing

process, and an unrealistic time table. The author of this thesis should have set more

realistic goals and timetable. Components being built by a student workforce take

longer due to classes and other time constraints. The author would like to say that he,

did all the work himself, but the author lacked a number of skills such as welding,

electronics expertise, and had to rely on others for help in these areas. Finding reliable

help to assist was difficult and asking the volunteers to give up more of their time to

help fabricate components quicker is a difficult task.   Volunteer work forces can only be

pushed so hard. Realistic goals need to be set because people who help out have other

projects that they need to work on as well.

Check Over Every Component on Arrival

The one horizontal linear actuator could have been exchanged for one that

extended the full length if it was known about in time. The horizontal linear actuator set

in its box from the time it was received until it was taken out for the first round of

testing. If the horizontal linear actuator was tested when it arrived, it could have been

exchanged in time.

Future Work

This tunnel is not at full analog operational readiness. There are a number of

improvements that need to be made before deployment for an analog mission. All of

these are small features, but will impact the ability of the operator to use the tunnel to

its full ability. The tunnel as it stands is operational but it can be improved. In the

methodology section the full improvements have been described as part of the original

design of the tunnel.

Upgrade Control Box

Finishing the control box will be done by installing the switch that reverses the polarity of the current to the linear actuators, and the lights for the contact sensors.

Weather Proofing System

In an analog mission as described in the introduction of this thesis, the tunnel has to deal with weather on Earth. There needs to be a weather proofing system to protect the integrity of the tunnel. This means protecting the mating rings, limiting dust build up in the guide rails, and protecting the inside of the tunnel.

Protect Mating Rings

There needs to be a system in place to protect the mating rings from dust build up or snow or ice buildup. Electric heating strips will be mounted on the non-contact area. When electric current is running through the strips, the resistors in the strips warm up, and thus warming up the metal of the rings to prevent ice buildup.   The mating rings will have to be cleaned every few days.

Protect inside of tunnel

To deal with dust build up, there will be a fabric door similar to those used in a tent, to keep the dust from the mating rings out of the transfer tunnel. There will also be metal doors on both ends of the tunnel and rover.

Upgrade Cart

The cart needs to be upgraded. It needs to extend more to move the center of gravity back to the center of the cart without the use of weights. When the cart is upgraded, the guide rail system will also be upgraded to include a bearing system that is self-contained so not to allow dust build up to affect it.

Latch System

The latch system will have to be integrated into the rover and the tunnel side mounting plates.

Rover Side control

There will have to be a way for the crew in the PER to control the tunnel. A type of wireless system should be designed to allow a signal to start an automated docking process.

Computer Controlled System

The final goal of this tunnel would be to have it run by an automated process. This will free up time for the crew and allow the tunnel to dock with the ILH or PER even if there is no one at the controls.

Bladder

The bladder is being designed and manufactured with the help of ILC Dover. Once finished, this bladder will need to be installed and integrated into the tunnel.

There needs to be an extendable floor to help with the transfer of crew and cargo.

TRL Levels

NASA uses a system called the Technology Readiness Level (TRL). This is a set of levels of technology advancement from an idea on a piece of paper to a spaceflight proven component.

Table 7: NASA TRL from http://esto.nasa.gov/files/TRL_definitions.pdf

Level	Name	Description
1	Basic principles observed and reported	Transition from scientific research to applied research. Essential characteristics and behaviors of systems and architectures. Descriptive tools are mathematical formulations or algorithms.
2	Technology concept and/or application formulated	Applied research. Theory and scientific principles are focused on specific application area to define the concept. Characteristics of the application are described. Analytical tools are developed for simulation or analysis of the application.
3	Analytical and experimental critical function and/or characteristic proof-of-concept	Proof of concept validation. Active Research and Development (R&D) is initiated with analytical and laboratory studies. Demonstration of technical feasibility using laboratory testing.
4	Component/subsystem validation in laboratory environment	Standalone prototyping implementation and test. Integration of technology elements. Experiments with full-scale problems or data sets.
5	System/subsystem/component validation in relevant environment	Thorough testing of prototyping in representative environment. Basic technology elements integrated with reasonably realistic supporting elements. Prototyping implementations conform to target environment and interfaces.
6	System/subsystem model or prototyping demonstration in a relevant end-to-end environment (ground or space)	Prototyping implementations on full-scale realistic problems. Partially integrated with existing systems. Limited documentation available. Engineering feasibility fully demonstrated in actual system application
7	System prototyping demonstration in an operational environment (ground or space)	System prototyping demonstration in operational environment. System is at or near scale of the operational system, with most functions available for demonstration

		and test.
8	Actual system completed and "mission qualified" through test and demonstration in an operational environment (ground or space)	End of system development. Fully integrated with operational hardware and software systems. Most user documentation, training documentation, and maintenance documentation completed. All functionality tested in simulated and operational scenarios. Verification and Validation (V&V) completed.
9	Actual system "mission proven" through successful mission operations (ground or space)	Fully integrated with operational hardware/software systems. Actual system has been thoroughly demonstrated and tested in its operational environment. All documentation completed. Successful operational experience. Sustaining engineering support in place.

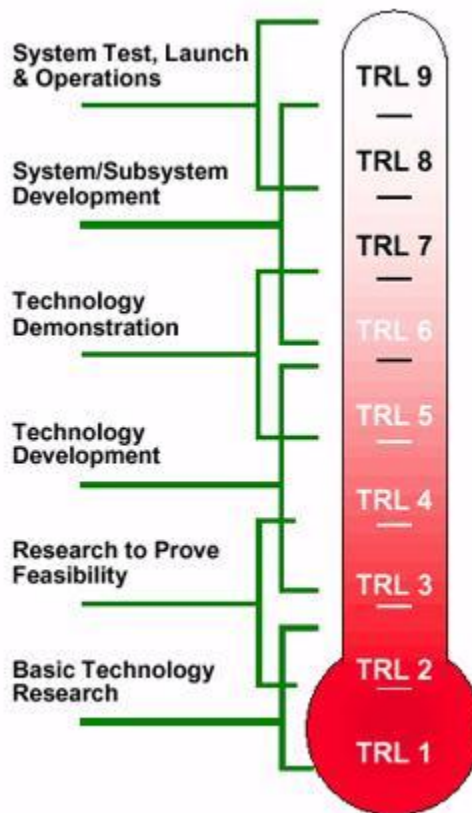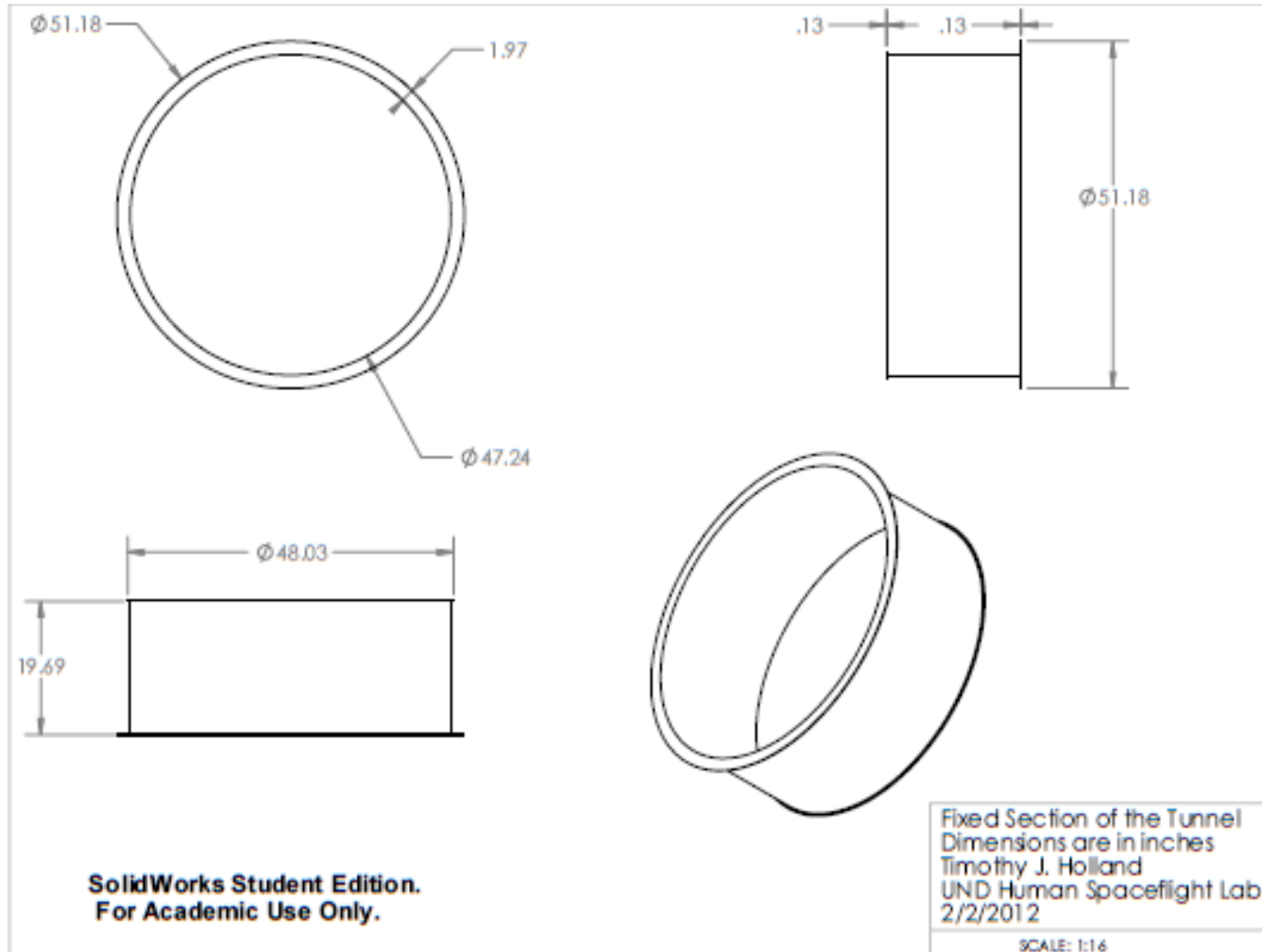Another way to view TRL is to look at Figure 62:

The entire project that the UND Human Spaceflight Lab under the NASA EPSCOR

grant is working on is only going to about a TRL of 6 to 7. This is because it is a concept
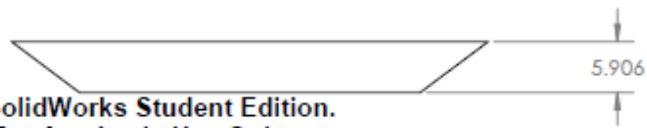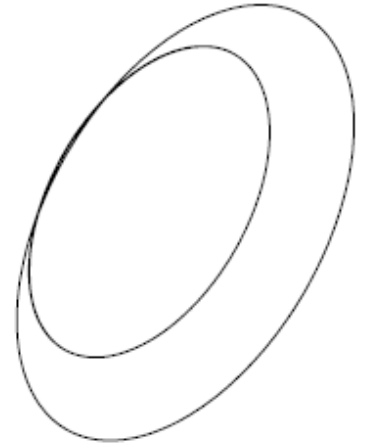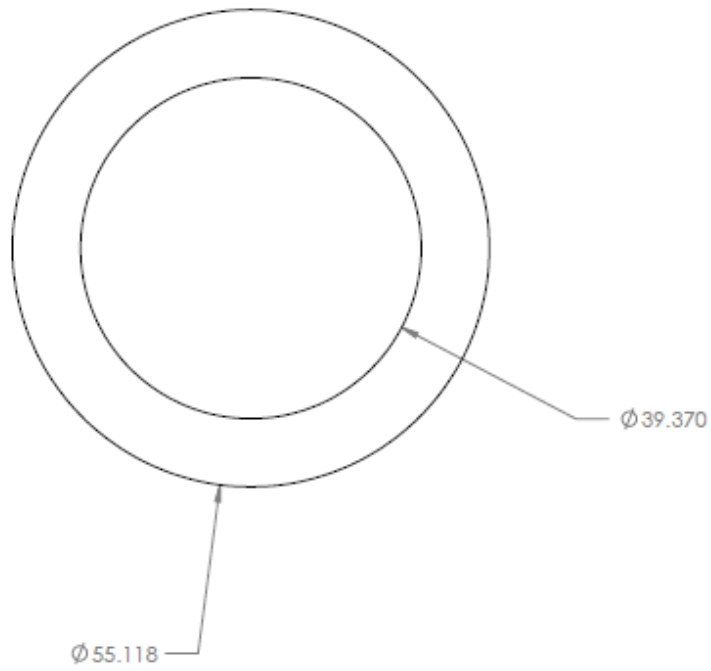
design project to prove that this integrated system is feasible. None of the systems

under development as part of the current NASA EPSCOR grant was supposed to be flight

ready hardware. This tunnel is not supposed to be flight ready, but ready for analog

testing. The tunnel that is being designed by this thesis is now at a TRL of about 5. The

tunnel is now going through system/subsystem/ component validation before it can

integrate into the ILH.

Most of the docking systems discussed in the introduction of this thesis have a

TRL of 9 because they are operational ready, mission tested hardware. A transfer

system similar to the one that this thesis designs and tests was not found in the

literature review for this thesis. Due to this factor it is difficult to compare an analog

transfer system to a space operational transfer system.

APPENDIX

Engineering Drawings

Ø51.18
1.97
.13 .13
Ø51.18
Ø47.24
Ø48.03
19.69

SolidWorks Student Edition.
For Academic Use Only.

Fixed Section of the Tunnel
Dimensions are in inches
Timothy J. Holland
UND Human Spaceflight Lab
2/2/2012

SCALE: 1:16

Ø 39.370

Ø 55.118

5.906

SolidWorks Student Edition.
For Academic Use Only.

Ring Design

DIMENSIONS ARE IN INCHES
Tim Holland
UND Human Space Flight Lab
11/17/2011

SCALE: 1:15

R1.600

15.613

R2.509

Ø55.118

56.000

Ø39.370

56.000

5.906
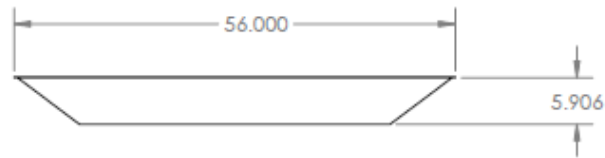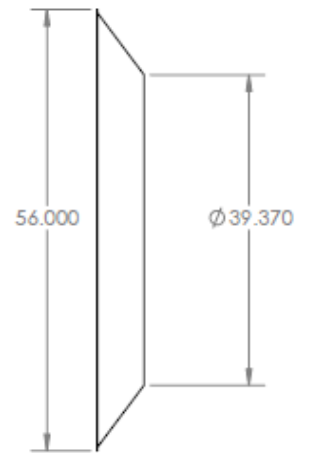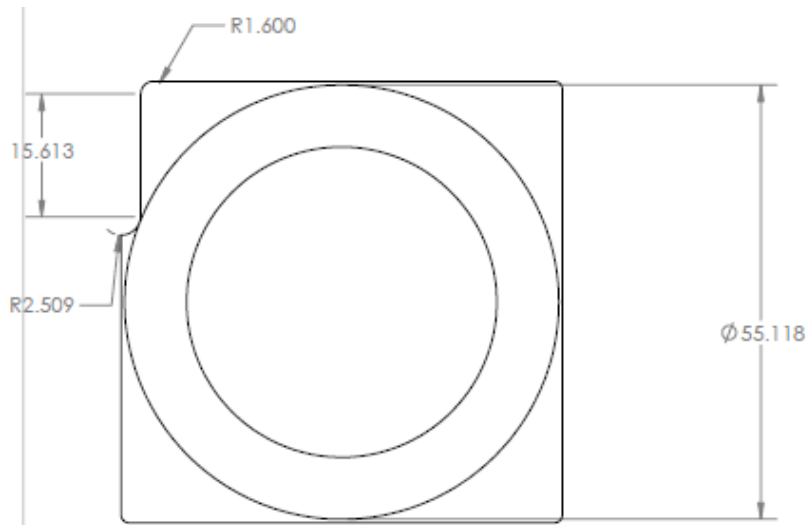
SolidWorks Student Edition.
For Academic Use Only.

Rover Side Ring Mounted on Plate
Dimensions are in inches
Tim Holland
UND Human Space Flight Lab
11/17/2011

SCALE: 1:16

Ø 55.118

43.472

Ø 39.410
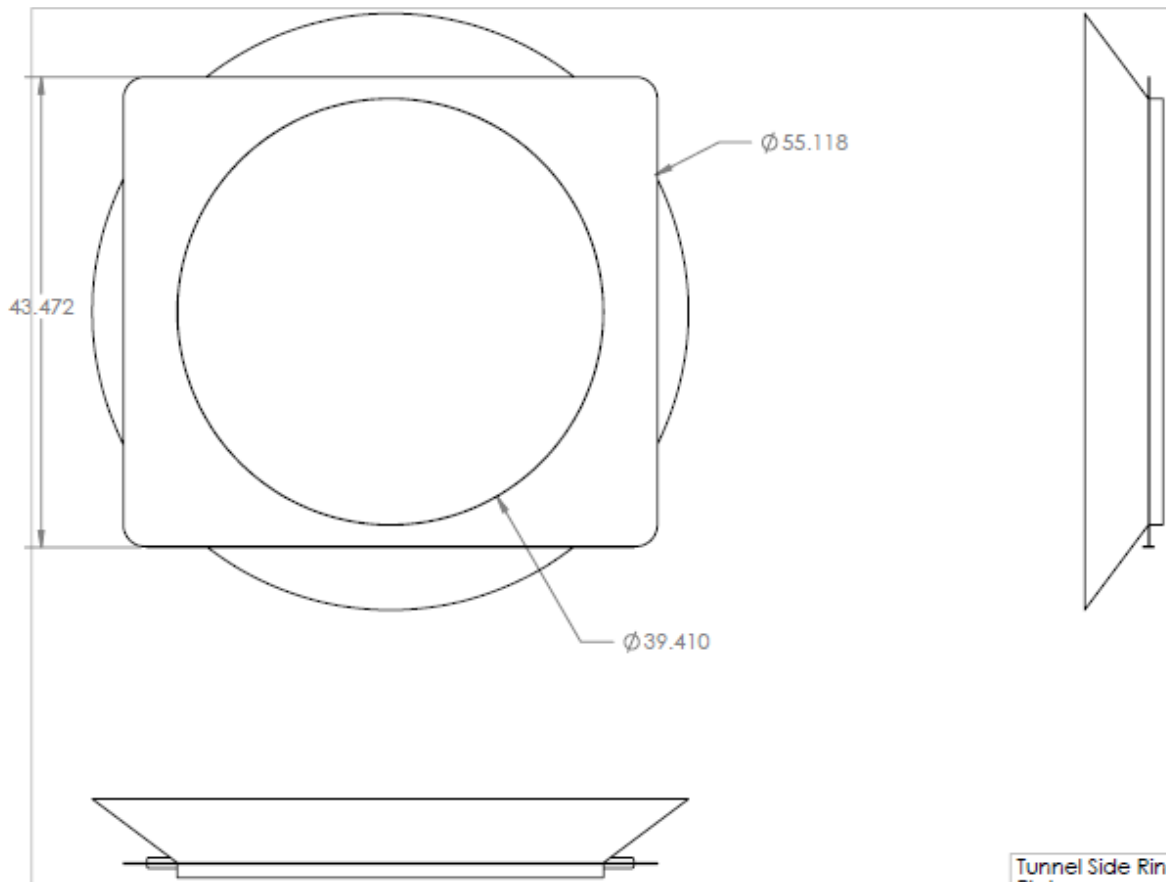
Tunnel Side Ring with Mounting Plate
Dimensions are in inches
Timothy J. Holland
UND Human Space Flight Lab
11/17/2011

SCALE: 1:12

Ø 39.410

1.250

Ø 39.410

.102

1.000

45.000

49.370

Tunnel Side Ring Mounting Plate
Dimensions are in inches
Timothy J. Holland
UND Human Space FLight Lab
11/17/201

SCALE: 1:8

Cart for Tunnel
Dimensions are in Inches
Timothy J. Holland
UND Human Spaceflight Lab
2/23/2012

SCALE: 1:16

SolidWorks Student Edition.
For Academic Use Only.

DETAIL A
SCALE 1 : 3

136

PART NAME	PLASTICASE	PART No.	PC-11495

MATERIAL: BODY TOP & BOTTOM, REAR PANEL _____ ABS THERMOPLASTIC (UL94-HB RATED)
        UPPER SLOPE PANEL _____ 0.063 THK. ALUMINUM
        LOWER SLOPE PANEL _____ 0.100 THK. ALUMINUM

FINISH: BODY TOP & BOTTOM _____ LIGHT GRAY
        REAR PANEL _____ DARK GRAY
        SLOPE PANELS _____ NATURAL

UPPER PANEL

REMOVABLE ALUMINUM PANELS (PRESSURE SENSITIVE TAPE ON ONE SIDE)

LOWER PANEL

4.965
2.550
1.862 MAX.
4.529 MAX.
15°
2.611 MAX.
1.180
1.380
8.500
1.483 MIN.
1.748 MIN.
1.975
10°

4.890
5.115

7.638 TYP.
7.864 TYP.
8.975

0.250 DIA. BOSS WITH 0.094 DIA. HOLE (7) PLACES

3.898 | 3.898

*8.125
*7.650
3.661
3.661
1.373
0.200
0.746

BODY BOTTOM
(WITH BODY TOP REMOVED)

3.543 | 3.543

FOUR (4) M3 x 0.630" LG. SCREWS SUPPLIED FOR ASSEMBLING BODY TOP TO BOTTOM

SIX (6) M3 x 0.315" LG. CSK. SCREWS SUPPLIED FOR ASSEMBLING SLOPE PANELS TO BODY TOP

FOUR (4) RUBBER STICK-ON FEET SUPPLIED

MOUNTING BOSSES USE EITHER M2.5 METRIC OR #4 STD. SHEET METAL SCREWS x 0.188" LG. (NOT SUPPLIED)

NOTE: ALL DIMENSIONS HAVE ±0.015 TOLERANCE UNLESS OTHERWISE SPECIFIED

* THESE INSIDE DIMENSIONS ARE TAKEN FROM CLOSED END OF THE BOX

1.250

7.510

REAR VIEW

REMOVABLE REAR PANEL 0.090 THICK (TEXTURED ON ONE SIDE)

137

1.0 BRAND:	
2.0 PRODUCT DESCRIPTION:	V-Grooved Wheel Casters

3.0 PRODUCT PHOTO(S):

POLYURETHANE SERIES
(1 NWC8, 1NWC9, 1NWD1-1NWD4)
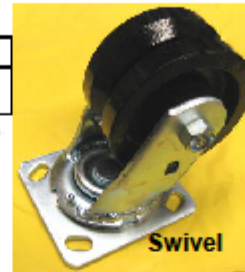
CAST IRON & FORGED STEEL SERIES

Swivel   Rigid

4.0 PRODUCT REQUIREMENTS:

4.1 Features & Performance	Requirement

Heavy Duty welded frame with 90° V-groove wheel can be used with angle iron track.
Uses: Moving Machinery, Production/Tow Line, and Controlled Path Movement.
(Note: If angle iron is used as a load-bearing track, it must be 1 ½" x 1 ½" profile heavy wall type.)
Features include:
- Double Race Ball Bearings on Swivel Casters
- Roller Bearings on Wheel Axle.
- Axle Zerk Grease Fittings on All Casters, and Swivel Race Grease Fittings on Swivel Casters.

Model No.	Load Rating (Lb.)	Caster Type	Overall Height (In.)	Wheel Dia. (In.)	Wheel Width (In.)	Wheel Model No.	Wheel Material & Color	Mounting Type	Mounting Bolt Size	Frame & Plate Material
1NWB2	800	Swivel	5 5/8	4	1 1/2	1NWB8	Cast Iron, Powder Coat Black Finish	15	3/8"	Minimum: (6 mm) Thick Steel, Zinc Plated
1NWB3	800	Rigid	5 5/8	4	1 1/2					
1NWB4	1200	Swivel	7 1/2	6	2	1NWB9		39	3/8"	
1NWB5	1200	Rigid	7 1/2	6	2					
1NWB6	1500	Swivel	7 1/2	6	2 1/2	1NWC1		43	1/2"	
1NWB7	1500	Rigid	7 1/2	6	2 1/2					
1NWC2	800	Swivel	5 5/8	4	2	1NWF9	Cast Iron, Powder Coat Black Finish	15	3/8"	Minimum: (6 mm) Thick Steel, Zinc Plated
1NWC3	800	Rigid	5 5/8	4	2					
1NWC4	900	Swivel	6 1/2	5	2	1NWG1				
1NWC5	900	Rigid	6 1/2	5	2					
1NWC6	1000	Swivel	7 1/2	6	2	1NWB9				
1NWC7	1000	Rigid	7 1/2	6	2					
1NWC8	350	Swivel	5 5/8	4	2	1NWG2	Molded Poly-urethane, Red	15	3/8"	Minimum: (6 mm) Thick Steel, Zinc Plated
1NWC9	350	Rigid	5 5/8	4	2					
1NWD1	400	Swivel	6 1/2	5	2	1NWG3				
1NWD2	400	Rigid	6 1/2	5	2					
1NWD3	450	Swivel	7 1/2	6	2	1NWG4				
1NWD4	450	Rigid	7 1/2	6	2					

This specification is based on the manufacturers design and is to be used as a Quality Control document.

Caster Model 1NWB3 is used in this thesis.

Bibliography

1728 Software Systems. (2012). *Basic Electricity*. Retrieved Feburary 27, 2012, from 1728 Software Systems: http://www.1728.org/project2.htm

American Institute of Steel Construction. (1989). *Manual of Steel Construction, Allowable Stress Design, 9th ed.* New York: American Institute of Steel Construction.

Bannova, O. (n.d.). *Terrestrial Analogs for Planetary Surface Facility Planning and Operations.* Houston: University of Houston Sasakawa International Center for Space Architecture.

Beer, F. P., Johnston, E. R., & DeWolf, J. T. (2003). *Mechanics of Materials.* New York: McGraw Hill.

Bruhn , E. (1973). *Analysis and Design of Flight Vehicle Structures.* Indianapolis, IN: S.R. Jacobs and Associetes, Inc.

Budynas, R. G. (1977). *Andvanced Strenght and Applied Stress Analysis.* New York: Mcgraw-Hill College.

Chambers, D., & Fischer, B. (2011, July 18). *Space Analog Testing*. Retrieved Feburary 15, 2012, from NASA.gov: http://www.nasa.gov/centers/johnson/engineering/integrated_environments/space_analog_testing/index.html

Cook, J., Aksamentov, V., Hoffman, T., & Bruner, W. (2011). *ISS Interface Mechanisms and their Heritage.* Houston: The Boeing Company.

eFunda, Inc. (2012). *Buckling of Columns*. Retrieved March 7, 2012, from eFunda: http://www.efunda.com/formulae/solid_mechanics/columns/intro.cfm

Fehse, W. (2003). *Automated Rendezvous and Docking of Spacecraft.* Cambridge: Cambridge Univeristy Press.

Gill, P. (n.d.). *How Does a Linear Actuator Work?* Retrieved 2 14, 2012, from eHow.com: http://www.ehow.com/how-does_5601089_linear-actuator-work_.html

Hall, R. D., & Shayler, D. J. (2003). *Soyuz: A Universal Spacecraft.* London: Praxis Publishing Ltd.

Howard, R. T., & Bryan, C. T. (2009). The Next Generation Advanced Video Guidance Sensor: Flight Heritage and Current Development. *Space, Propulsion & Energy Sciences International Forum-SPESIF-2009* (pp. 615-621). American Institute of Physics.

Howard, R. T., & Carrington, C. K. (2008). Multi-Sensor Testing for Automated Rendezvous and Docking. *Space Technology and Applications International Forum-STAIF 2008* (pp. 725-732). American Institute of Physics.

Kauderer , A., & Dunbar, B. (2011, April 1). *About NEEMO*. Retrieved Feburary 15, 2012, from NASA.gov: http://www.nasa.gov/mission_pages/NEEMO/about_neemo.html

Kennedy, K., Toups, L., & Smitherman, D. (2007). *Lunar Habitation Strategies.* Washington D.C.: NASA.

Lee, P., & Lorber, K. (2010, August 20). *Haughton-Mars Project*. Retrieved Feburary 15, 2012, from Mars On Earth: http://www.marsonearth.org/

Loff , S., & Lind, R. (2011, May 22). *About Analog Missions And Field Tests*. Retrieved Feburary 15, 2012, from NASA.gov: http://www.nasa.gov/exploration/analogs/about.html

Loff , S., & Lind, R. (2011, 7 14). *Pavilion Lake Team Explores the Deep to Learn More about Life and Science*. Retrieved Feburary 15, 2012, from NASA.gov: http://www.nasa.gov/exploration/analogs/about_pavilionlake.html

Loff , S., & Lind, R. (2012, January 20). *Desert RATS*. Retrieved Feburary 15, 2012, from NASA.gov: http://www.nasa.gov/exploration/analogs/desertrats/index.html

Loff , S., & Lind, R. (2009, 7 28). *Past and Present: Field Testing For the Moon*. Retrieved Feburary 15, 2012, from NASA.gov: http://www.nasa.gov/exploration/analogs/then-and-now.html

Marquez, J. J., & Newman, D. J. (2006). Mission Planning and Re=planning for Planetary Extravehicular Activities: Analysis of Excursions in a Mars-Analog Environment and Apollo Program. *SAE International*, 2006-01-2297.

Mastascusa, E. J. (2002). *An Introduction To Control Systems*. Retrieved Feburary 21, 2012, from Welcome To Exploring Classical Control Systems : http://www.facstaff.bucknell.edu/mastascu/econtrolhtml/Intro/Intro1.html

Mitchell, J. D., Cryan, S. P., Baker, K., Martin, T., Goode, R., Key, K. W., et al. (2008). Intergated Docking Simulation and Testing with the Johnson Space Center Six-Degree-of-Freedom Dynamic Test System. *Space Technology and Applications International Forum-STAIF 2008* (pp. 709-716). American Institute of Physics.

Morovision Night Vision, Inc. (n.d.). *HOW THERMAL IMAGING INFRARED TECHNOLOGY WORKS*. Retrieved Feburary 15, 2012, from MoroVision: http://www.morovision.com/how_thermal_imaging_works.htm

Mosher, D. (2007, July 7). *Future Mars Explorers Face Dusty Challenges*. Retrieved November 10, 2011, from Space.com: http://www.space.com/4051-future-mars-explorers-face-dusty-challenges.html

NASA. (1995). *Man-system Intergration Standards NASA-STD-3000.* NASA.

NASA. (1995). *Man-System Integration Standards. NASA-STD-3000.* NASA.

NASA. (2000, August 31). *GUIDANCE, NAVIGATION AND CONTROL*. Retrieved Feburary 22, 2012, from NSTS Shuttle Reference Manual (1988): http://science.ksc.nasa.gov/shuttle/technology/sts-newsref/sts-gnnc.html

NASA. (2010). *HUMAN INTEGRATION DESIGN HANDBOOK: NASA/SP-2010-3407.* Washington D.C.: NASA.

Palmisano, J. (2005). *ACTUATORS - SOLENOIDS*. Retrieved March 9, 2012, from Society of Robots: http://www.societyofrobots.com/actuators_solenoids.shtml

Parxy. (n.d.). *How Laser Pointers Work*. Retrieved Feburary 15, 2012, from Parxy.com: http://www.parxy.com/how-pointers-work.html

Roe, F. D., & Howard, R. T. (2003). The Succesful Developement of an Automated Rendezvous and Capture (AR&C) System for the National Aeronautics and Space Administration. *Space Technology and Applications International Forum-STAIF 2003* (pp. 313-319). American Institute of Physics.

Ruess, F., Schaenzlin, J., & Benaroya, H. (2006). Structural Design of a Lunar Habitat. *Hournal of Aerospace Engineering*, 133-157.

Society of Robots. (2005). *SENSORS - SHARP IR RANGE FINDER*. Retrieved 2 15, 2012, from Society of Robots: http://www.societyofrobots.com/sensors_sharpirrange.shtml

Sokolnikoff, I. (1983). *Mathematical theory of elasticity.* Malabar FL: Krieger.

Thaller, M. (n.d.). *Teachers Guide to the Infrared*. Retrieved Feburary 15, 2012, from Cool Cosmos: http://coolcosmos.ipac.caltech.edu/image_galleries/ir_zoo/lessons/background.html

Toups, L., & Kennedy, K. J. (2009). *Constellation Architecture Team-Lunar.* Houston: NASA.

Tyson, J. (n.d.). *How Scanners Work*. Retrieved 2 15, 2012, from HowStuffWorks: http://computer.howstuffworks.com/scanner1.htm

van Brook, L. (2010). *Basic requirments of life support of a hybrid Inflatable Terrestrial Habitat as a Frist Step in Lunar Habitation Strategies.* Grand Forks: Univeristy of North Dakota, Department of Space Studies.

Xavier, C., Sun-Wook, K., Michel, I., Arun, M., & Gilbert, J. (1995). Post-Impact Dynamics of Two Multi-Body Systems Attempting Docking/Berthing. *Acta Astronautica*, 729-769.

Yang, Z., Hao, T., & Qiu-sheng, W. (2007). Analysis of dynamometry scheme for semi-physical simulation platform of space docking mechanism. *Advances in Engineering Software*, 710-716.

Yaskevich, A. (2006). Combined Equations of Motion for Description of Dynamics of Spacecraft Docking Using the Pin-Cone System. *Cosmic Research*, 305-316.